Influence of initial soil moisture in a Regional Climate Model study over West Africa. Part 2: Impact on the climate extremes.

Brahima KONÉ[1], Arona DIEDHIOU[1, 2], Adama Diawara[1], Sandrine Anquetin[2], N'datchoh Evelyne Touré[1], Adama Bamba[1] and Arsene Toka Kobea[1]

[1]LAPAMF, Université Félix Houphouët Boigny, Abidjan, Côte d'Ivoire

[2]Univ. Grenoble Alpes, IRD, CNRS, Grenoble INP, IGE, F-38000 Grenoble, France

Correspondence to: Arona DIEDHIOU (arona.diedhiou@ird.fr)

Abstract.

The influence of the initial soil moisture conditions on extreme climate extreme over West Africa was investigated using the fourth generation of Regional Climate Model version 4 (non-hydrostatic) coupled to the version 4.5 of the Community Land Model (RegCM4-CLM4.5) at 25 km spatial resolution. Sensitivity studies were performed for five years (2001-2005), with initial soil moisture conditions prescribed on June 1 and simulations performed over four months (120 days) from June to September (JJAS). The Results were presented for two extreme years 2003 (above normal precipitation year) and 2004 (below normal precipitation year) to estimate the impact limits of internal forcing of initial soil moisture on the new non-hydrostatic dynamical core of RegCM4. We initialized the control runs with the reanalysis soil moisture of the European Centre Meteorological Weather Forecast's reanalysis of the 20th century data (ERA20C), while for the dry and wet experiments, we initialized the soil moisture at the maximum and minimum value over West Africa studied domain, respectively. The impact on extreme precipitation indices of the initial soil moisture, especially over the central Sahel, is linear; that is, dry (wet) experiments decrease (increase) precipitation extreme indices only for precipitation indices related to the number of precipitation events, not for those related to the event intensity. Initial soil moisture conditions unequally affect the daily minimum and maximum temperatures. A stronger impact is found on the maximum temperature than the minimum temperature. Over the entire West African domain, wet (dry) experiments cause a decrease (increase) in maximum temperature. The impact of initial soil moisture conditions on the indices related to the minimum temperature (TNx and TNn indices) is linear only for TNx index over central Sahel, that is, dry (wet)

experiments cause an increase (a decrease) in the TNx index. The performance of RegCM4-CLM4.5 in simulating the ten extreme rainfall and temperature indices used in this study are also highlighted.

1 Introduction

West Africa experienced large rainfall variability during the late 1960s. This variability often leads to flooding events, severe drought, and regional heatwaves, which have major economic, environmental, and societal impacts (Easterling et al., 2000; Larsen, 2003). In recent years, climate extremes have attracted much interest because they are expected to occur more frequently (International Panel on Climate Change (IPCC), 2012) than changes in the mean climate. Yan and Yang (2000) showed that for many cases, the extreme climate changes were five to ten times greater than climate mean change. Many key factors or physical mechanisms could be the cause of the increase in climate extremes (Nicholson, 1980; Le Barbé et al., 2002), such as the effect of increasing greenhouse gases in the atmosphere on the intensification of hot extremes (IPCC, 2007), sea surface temperature (SST) anomalies (Fontaine and Janicot 1996; Folland et al., 1986), and land surface conditions (Philippon et al., 2005; Nicholson (2000)). In addition, smaller-scale physical processes, including the interactions of land–atmosphere coupling, can lead to changes in climate extremes. For the European summer, the influence of soil moisture on land–atmosphere coupling using a regional climate model and focused on the extremes and trends in precipitation and temperature have been studied by Jaeger and Seneviratne (2011). For extreme temperatures, their studies have shown that interactions of soil moisture and climate have a significant impact, while for extreme precipitation, they only influence the frequency of wet days. Over Asia, Liu et al. (2014) studied the impact on subsequent precipitation and temperature of soil moisture anomalies using a regional climate model. They showed that wet (dry) experiences decrease (increase) the hot extremes, decrease (increase) the drought extremes, and increase (decrease) the cold extremes in a zone with strong soil moisture–atmospheric coupling. However, none of these studies examined the impacts of the initial soil moisture conditions on subsequent climate extremes using a regional climate model over West Africa. In part 1, the influence of initial soil moisture on the climate mean was based on a performance assessment of the Regional Climate Model coupled with the complex Community Land Model (RegCM4-CLM4.5) performed by Koné et al. (2018), where the ability of the model to

reproduce the climate mean has been validated. In Part 2, before starting to study the influence of initial soil moisture on climate extremes, it was necessary to assess the performance of RegCM4-CLM4.5 in simulating the ten (10) indices of temperature and precipitation extremes used in this study. This has never been done before in West Africa with this version of RegCM with a non-hydrostatical scheme; therefore, we separated the work in two parts, a first one assessing the ability of the model to simulate the climate extreme indices, and a second one investigating how and what is the time limit of the effect of initial soil moisture condition on the magnitude or duration of these climate extremes. The manuscript is organized as follows: Section 2 describes the RegCM4 model, the experimental design, and the methodology used in this study; Section 3 presents results of the two parts of the work and Section 4 documents the main conclusions.

2. Model, experimental design and methodology

2.1 Model description and numerical experiment

The fourth generation of the Regional Climate Model (RegCM4) of the International Centre for Theoretical Physics (ICTP) is used in this study. Since this version, physical representations have been subject to a continuous process of implementation and development. The release used in this study was RegCM4.7. The non-hydrostatic dynamical core of the MM5 (Mesoscale Model version 5, Grell et al., 1994) was ported to RegCM4 while maintaining the existing hydrostatic core. RegCM4 is a limited-area model using a vertical grid sigma hydrostatic pressure coordinate and a horizontal grid of the Arakawa B-grid (Giorgi et al., 2012). The radiation scheme is from the NCAR-CCM3 (National Center for Atmospheric Research and the Community Climate Model Version 3) (Kiehl et al., 1996), and the aerosol representation is from Zakey et al. (2006) and Solmon et al. (2006). The large-scale precipitation scheme used in this study is from Pal et al. (2000); the moisture scheme is called the SUBgrid EXplicit moisture scheme (SUBEX), which considers the sub-grid variability in clouds. The accretion and evaporation processes for stable precipitation are from Sundqvist et al. (1989). The sensible heat and water vapour in the planetary boundary layer over land and ocean, as well as the turbulent transport of momentum, is reported by Holtslag et al. (1990). The heat and moisture and momentum of ocean surface fluxes are from Zeng et al. (1998). Convective precipitation and land surface processes in RegCM4.7 are represented in several options. Based on Koné et al. (2018), the convective scheme of Emanuel (1991) is used. The parameterization of land surface processes is from CLM4.5 (Oleson et al., 2013). In

96   each grid cell of CLM4.5, there are sixteen different plant functional types and ten soil layers
97   (Lawrence et al., 2011; Wang et al., 2016). The integration of RegCM4 over the West African
98   domain is shown in Fig. 1 with eighteen vertical levels and 25 km of horizontal resolution
99   (182×114 grid points; from 20°W–20°E and 5°S–21°N). The European Centre for Medium-
100 Range Weather Forecasts reanalysis (EIN75; Uppala et al., 2008; Simmons et al., 2007)
101 provides the initial and boundary conditions. The sea surface temperatures (SSTs) are derived
102 from the National Oceanic and Atmosphere Administration optimal interpolation weekly
103 (NOAA; OI_WK) (Reynolds et al., 1996). The topography is derived from the United States
104 Geological Survey (USGS) Global Multi-resolution Terrain Elevation Data (GMTED;
105 Danielson et al., 2011) at a spatial resolution of 30 arc-s, which is an update of the Global
106 Land Cover Characterization (GTOPO; Loveland et al., 2000) dataset.

107 The initial soil moisture sensitivity does not exceed four months (Hong and Pan., 2000; Kim
108 and Hong, 2006). (Hong and Pan., 2000; Kim and Hong, 2006). As mentioned in Part I, we
109 performed sensitivity studies on the initial soil moisture conditions over the West African
110 domain for June–July–August–September (JJAS) from 2001 to 2005 with a focus on two
111 contrasting years, 2003 (above normal precipitation year) and 2004 (below normal
112 precipitation year). The two years, 2003 and 2004 (respectively, the wettest and driest years
113 among the five years), were selected to estimate the limits of the impact of internal soil
114 moisture forcing on the new non-hydrostatic dynamical core of RegCM4. Several previous
115 studies used two extreme years for their sensitivity study of initial soil moisture conditions on
116 the models (e. g., Hong et al., 2000; Kim and Hong, 2006). We set up an ensemble of three
117 experiments, each with simulations starting from June 1 to September 30. For each
118 experiment, we applied (i) a reference initial soil moisture condition, (ii) a wet initial soil
119 moisture condition, and (iii) a dry initial soil moisture condition. Kang et al. (2014) compared
120 different land surface schemes (BATS and CLM3) and different spin-up periods to simulate
121 June–July–August precipitation and recommended a 7-day spin-up period. In this study, we
122 used CLM4.5 as the land surface scheme (Oleson et al., 2013), which has a more complex
123 design. The first seven days (Kang et al., 2014) were excluded from the analysis as a spin-up
124 period. We used the soil moisture from the reanalysis of the European Centre Meteorological
125 Weather Forecast's Reanalysis of the 20th century (ERA20C) to initialize the control runs.
126 Wet and dry experiments were initialized for the soil moisture (in volumetric fraction m3•m-

127   3) at the maximum (= 0.489) and minimum (= 0.117.10-4) soil moisture values over West

128   Africa derived from the ERA20C soil moisture dataset.

2.2 Validation datasets and evaluation metrics

130   Our investigation focused on the air temperature at 2 m and the precipitation over the West

131   African domain during JJAS for 2003 and 2004. The simulated precipitation fields are

132   validated with two observation datasets: the Climate Hazards Group Infrared Precipitation

133   Stations (CHIRPS) dataset from the University of California at Santa Barbara, available from

134   1981 to 2020 with 0.05° high-resolution data and the Tropical Rainfall Measuring Mission

135   3B43V7 (TRMM) dataset with 0.25° high-resolution data available from 1998 to 2013

136   (Huffman et al., 2007). We validated the 2-m temperature using two observation datasets: the

137   NOAA CPC global daily temperature from the Global Telecommunication System (GTS),

138   gridded at a horizontal resolution of 0.5° from 1979 to 2020 (Fan Y. and Huug van den Dool,

139   2008), and daily temperature from ERA-Interim (EIN) reanalysis at 0.25° of horizontal

140   resolution available from 1979 to 2020 (Dee et al., 2011). To compare the model simulations

141   with the observation datasets, we re-gridded all the products to 0.22° × 0.22° using a bilinear

142   interpolation method (Nikulin et al., 2012).

143   The performance of RegCM4-CLM4.5 to simulate the extreme indices was evaluated using

144   four selected sub-regions (Fig. 1) based on the previous work of Koné et al. (2018), which

145   correspond to different annual precipitation cycle features. We used the mean bias (MB),

146   which captures the small-scale differences between the simulation and observation. The

147   pattern correlation coefficient (PCC) is also used as a spatial correlation between model

148   simulations and observations to indicate the large-scale similarity degree.

149   To quantify the impact of soil moisture anomalies on climate extremes, in their work over

150   Asia, Liu et al. (2014) used the MBs in five subregions. In our study, we used the MBs and

151   the probability density functions (PDF, Gao et al. (2016); Jaeger and Seneviratne (2011)) for

152   this purpose to better capture how many grid points are impacted by initial soil moisture and

153   their highest value.

154   Significance of differences was tested for the control vs. sensitivity experiments. We used a

155   two-tailed Student's t-test at each grid point as in Liu et al. (2014) over Asia. Owing to the

156   multiplicity problem of independent tests and the spatial dependency of neighboring! grid

157   points, the significant results can only be seen as a crude estimate. Therefore, we perform the

158 land point area-weighted fraction with a statistical significance of 10% and display the

159 seasonal extreme indices maps for 2003 and 2004.

160

161 **2.3. Extreme rainfall and temperature indices**

162 In this study, to investigate the changes in precipitation and temperature in terms of duration,

163 occurrence, and intensity, six extreme temperature and four extreme rainfall indices were

164 examined using daily minimum and maximum temperature and daily rainfall data (Table 1).

165 These ten extreme indices are recommended by the Expert Team on Climate Change

166 Detection and Indices (ETCCDI, Peterson et al., 2001). We estimated the monthly values of

167 the indices, which allowed us to investigate seasonal variations.

168 **3. Results and discussion**

169 **3.1. Seasonal extreme rainfall**

170 In this section, we analyse six extreme rainfall indices based on daily precipitation in

171 RegCM4 simulations over West Africa. All precipitation indices were calculated for JJAS in

172 2003 and 2004. Table 2 summarizes the PCC and the MB of all precipitation indices studied

173 in this section for TRMM observation and model simulations derived from control

174 experiments with reanalysis of the initial soil moisture ERA20C with respect to CHIRPS

175 observations, calculated for the west Sahel, central Sahel, Guinea coast, and the entire West

176 African domain during JJAS 2003 and 2004.

177

178 **3.1.1 The index of the number of the wet days (R1mm index)**

179 Figure 2 shows the mean values of the number of wet days (R1mm index, in days) from

180 CHIRPS (Fig. 2a, d) and TRMM (Fig. 2b, e) observations and their corresponding simulated

181 control experiments (Fig. 2c, f) with the initial soil moisture derived from ERA20C

182 reanalysis. We have chosen CHIRPS because of its high resolution, mainly because this

183 product has been widely assessed and used for the study of extreme events in West Africa by

184 Bichet et al. (2018a, b) and Didi et al. (2020). The two observation datasets CHIRPS (Fig. 2a,

185 d) and TRMM (Fig. 2b, e) show a similar large-scale pattern over the West African domain

186 with a PCC up to 0.98 (Table 2). The maximum values of the R1mm index were located over

187 mountainous regions such as the Cameroon Mountains, Jos Plateau, and Guinea Highlands,

188 while the minimum values of the R1mm index were found over the Sahel with the number of

189 wet days decreasing gradually from south to north. However, although the large-scale patterns

were similar, at the local scale, some differences were found in terms of the magnitude and spatial extent of these maxima and minima. The TRMM datasets underestimated the number of wet days over the central and west Sahel, and they were overestimated over the Guinea coast for both JJAS 2003 and JJAS 2004 (Table 2). A strongest underestimation was observed over the central Sahel with MB of approximately -6.76 and -7.51 days for JJAS 2003 and JJAS 2004, respectively (Table 2). However, the strongest overestimation was found over the Guinea coast with MB reached 8.89 and 10.44 days for JJAS 2003 and JJAS 2004, respectively (Table 2).

The control experiments (Fig. 2c, f) reproduced well the large-scale structure of the observed rainfall, with PCC values of 0.96 and 0.95 for JJAS 2003 and JJAS 2004, respectively (Table 2) over the entire West African domain, but did exhibit some spatial extent and magnitude biases at the local scale. The control experiment displayed a large and quite homogeneous area of maximum values of the R1mm index below 12° N latitude. The control experiments overestimate the number of wet days over most of the studied domains (Table 2). The largest MBs were found over the Guinea coast with MB more than 53.16 and 55.46 days for JJAS 2003 and JJAS 2004, respectively (Table 2). This overestimation of the number of wet days in RegCM4 was also found by Thanh et al. (2017) with RegCM4 for Asia.

Figure 2 (second panel) displays additional changes in the R1mm index for JJAS 2003 and JJAS 2004 for dry (Fig. 2g and i, for JJAS 2003 and JJAS 2004, respectively) and wet experiments (Fig. 2h and j, for JJAS 2003 and JJAS 2004, respectively) compared to their associated control experiments; the dotted area shows changes with statistical significance at the 10% level. The dry experiments (Fig. 2g, i) decrease the R1mm index while the wet experiments (Fig. 2h, j) favour an increase in the R1mm index, especially over central Sahel and a small part of west Sahel. The impact of initial soil moisture on R1mm was linear over central Sahel. However, over the Guinea coast sub-region, both wet and dry experiments showed a significant increase in R1mm.

For a better quantitative evaluation, Fig. 3 displayed the PDF distributions of the changes in the R1mm index over the studied domains (Fig. 1), during JJAS 2003 and 2004. Table 4 summarizes the maximum values of changes obtained on the PDF's for extreme precipitation indices used in this study. The results essentially confirmed the linear impact found over central Sahel (Fig. 3a). Over west Sahel, the Guinea coast, and the West African domain (Fig. 3b, c, and d), both dry and wet experiments led to an increase in the R1mm index. The

strongest R1mm index increase (decrease) was observed in wet (dry) experiments over west (central) Sahel, with a maximum change of approximately 12 days (-5.19 days) for JJAS 2003 (Table 4).

Summarizing the results of this section, RegCM4 overestimates the number of wet days over most of the studied domains. A linear impact on the R1mm index for the dry (wet) experiments was found over the central Sahel, with a decrease (increase) in R1mm index. These results were compatible with previous work that sustained a strong land–atmosphere coupling in areas between wet and dry climate regimes (Zhang et al., 2011; Koster et al., 2006. The strongest R1mm index increase (decrease) was observed in wet (dry) experiments over west (central) Sahel, with a maximum change of approximately 12 days (-5.19 days) for JJAS 2003.

3.1.2 Simple daily intensity index (SDII).

We analyzed in this section the SDII index which gives the amount of precipitation mean on wet days (daily precipitation >1mm). Figure 4 (first panel) is the same as Fig.2 (first panel) but shows the amount of precipitation mean on wet days (SDII index, in mm.day^{-1}). Over the entire West African domain, the two observations products CHIRPS (Fig.4a, d) and TRMM (Fig.4b, e) presented a similar large-scale pattern with a PCC about 0.86 for both JJAS 2003 and JJAS 2004 (Table 2). However, the maxima SDII index values are quite different in term of spatial extension and magnitude. Over the coastline of the Gulf of Guinea, CHIRPS datasets (Fig.4a, d) depicted the highest values of SDII index, more than 25 mm.day^{-1}. While the SDII index values, in TRMM datasets not exceed 12 mm.day^{-1} over most part of this region. Over the central and west Sahel, TRMM datasets showed large sparse values of SDII index up to 20 mm.day^{-1}, while CHIRPS datasets not exceed 12 mm.day^{-1} for both JJAS 2003 and JJJAS 2004. The largest underestimations of TRMM dataset with respect to CHIRPS were found over the Guinea coast sub-region with MB more than -5.24 and -6.44 mm.day^{-1} (for JJAS 2003 and JJAS 2004, respectively; Table 2). However, strongest overestimations were observed over central Sahel with MB reaching 3.67 and 2.07 mm.day^{-1} (for JJAS 2003 and JJAS 2004, respectively; Table 2).

The control experiments (Fig. 4 c, f) reproduced well the large-scale pattern of observation products with a PCC reaching 0.73 and 0.77 (in JJAS 2003 and JJAS 2004, respectively; Table 2) over the West African domain. However, at the local scale, some biases were observed. Over most of the studied domains, the magnitude of the SDII was underestimated,

255 not exceeding 10 mm•day-1, except over the Cameroon Mountains (Fig. 4c, f). Therefore,

256 precipitation events were less extreme in the control experiments. The largest MBs were

257 located over the Guinea coast with MBs more than −13.62 and −14.65 mm•day-1 (for JJAS

258 2003 and JJAS 2004, respectively; Table 2).

259 Figure 4 (second panel) is the same as Fig. 2 (second panel), but the display changes in the

260 amount of mean precipitation on wet days. Unlike the R1mm index, a change in the SDII was

261 not linear over most of studied domains. In general, a similar mixture of both increase and

262 decrease is shown for dry and wet experiments over most of the studied domains (Fig. 4,

263 second panel).

264 Figure 5 displays PDFs of changes in SDII, as in Fig. 3. The PDFs showed a maximum

265 change value centered approximately on zero (Table 4), indicating that change in the amount

266 of mean precipitation on wet days for wet and dry experiments is not significant.

267 In summary, RegCM4 underestimated the amount of mean precipitation on wet days over all

268 the domain studies. It is worth noting that precipitation events simulated by RegCM4 with the

269 current parameterization were less extreme, and the SDII did not exceed 10 mm.day^{-1} over the

270 entire West African domain. The impact of precipitation amount on wet days of the dry and

271 wet experiments is not significant and is not sensitive to the contrast of year over the entire

272 studied domain.

273 **3.1.3 Maximum number of consecutive dry days (CDD index).**

274 The duration of consecutive dry days (CDD index), which represents the maximum number of

275 consecutive dry days with precipitation less than 1 mm.day^{-1} was analyzed in this section.

276 Figure 6 (first panel) is the same as Fig. 2 (first panel) but shows the maximum number of

277 CDD (in days). CHIRPS datasets located the largest CDD index values over the Sahara, more

278 than 50 days (Fig. 6a, d). The lowest values were found over the Guinea coast, with CDD

279 index values, less than 8 days. Over the West African domain, both the CHIRPS and TRMM

280 datasets showed quite similar large-scale features over the entire West African domain with

281 PCC more than 0.92. However, at the local scale, the observation datasets exhibited some

282 disparities. In general, these disparities related only to the spatial extent, especially over the

283 Sahel region. In JJAS 2003, the band of CDD index values was in the range of [10; 20] days

284 and extended farther into the Sahel region for TRMM than CHIRPS. For JJAS in 2004,

285 TRMM observations (Fig. 6b, e) presented a narrower band of minimum CDD index values

286 over the Guinea coast around latitude 10° N than CHIRPS, which extended over the Guinea

287 coast. TRMM observations underestimated the CDD index over the entire West African

288 domain, with MB approximately −2.29 and −1.75 days (for JJAS 2003 and JJAS 2004,

289 respectively; Table 2).

290 The control experiments (Fig. 6c, f) over the entire West African domain, reproduced well the

291 large-scale pattern of the observed rainfall with a PCC more than 0.85 and 0.89 (for JJAS

292 2003 and JJAS 2004, respectively; Table 1). However, in terms of magnitude, some

293 differences were observed at the local scale. In general, the control experiments overestimated

294 the CDD index over most studied domains, except over the Guinea coast (Table 2). A

295 strongest overestimation CDD index was observed over west Sahel with MB reaching more

296 than 14.49 and 17.51 days (for JJAS 2003 and JJAS 2004, respectively; Table 2). The current

297 model parameterization increase the drought extreme over most of the studied domains,

298 except over the Guinea coast (Table 2).

299 Figure 6 (second panel) is the same as Fig. 2 (second panel) but shows changes in the

300 maximum lengths of consecutive dry spells (through the CDD index). The initial soil moisture

301 impact on CDD index was linear over the central and west Sahel (Fig. 6, second panel), and

302 the dry (wet) experiments increase (decrease) the maximum lengths of consecutive dry spells

303 (CDD index). However, particularly over the Guinea coast, the dry and wet experiments led

304 to a decrease in CDD index.

305 Figure 7 is the same as Fig. 3 but displays the PDF distribution of the changes in the CDD

306 index. The impact on the CDD index was linear over the central and west Sahel. A strongest

307 increase (decrease) in the CDD index was observed over the central (west) Sahel in dry (wet)

308 experiments with maximum change value reaching 3.80 (-12.73) days in JJAS 2004 (2003)

309 (Table 4).

310 In summary, RegCM4 overestimates the maximum number of consecutive dry days over most

311 studied domains, except over the Guinea coast. The linear impact on CDD index was

312 observed over the central and west Sahel, however, over the Guinea coast, the dry and wet

313 experiments led to a decrease in CDD index.

314 **3.1.4 Maximum number of consecutive wet days (CWD index).**

315 The persistence of wet spells (CWD index) which represents the maximum number of

316 consecutive wet days with precipitation ≥ 1 mm.day^{-1} is investigated in this section. Figure 8

317 (first panel) is the same as Fig.2 (first panel) but shows the CWD index. The observation

318 products TRMM (Fig.8b, e) and CHIRPS (Fig.8a, d) depicted a similar large-scale pattern

319 with the PCCs reached 0.90 and 0.87 (resp. for JJAS 2003 and JJAS 2004, Table 2). CHIRPS

320 observation located the maximum of CWD index over the mountain regions such as

321 Cameroon Mountains, Jos plateau and Guinea highlands and it is more than 20 days. While

322 the minimum values of CWD index were found over most of the area above the latitude 17°N

323 and did not exceed 4 days (Fig.8a, d). In general, the differences between TRMM and

324 CHIRPS observation concerned the maxima magnitude and its extent, which are more

325 pronounced in TRMM than CHIRPS. Generally, TRMM overestimated the CWD index over

326 most of the studied domains compared to CHIRPS, except over central Sahel (Table 2). The

327 strongest overestimation was found over the Guinea coast region with MB more than 2.47 and

328 2.38 days (resp. for JJAS 2003 and JJAS 2004, Table 2).

329 The control experiments well reproduced the large-scale pattern over the entire West African

330 domain, with PCCs values approximately 0.81 and 0.87 (resp. for JJAS 2003 and JJAS 2004,

331 Table 2). However, at the local scale the control experiments exhibit some biases in the

332 minimum and maximum CWD index values in term of magnitude and spatial extent. Control

333 experiments overestimated the CDD index over most of domains studied (Fig. 8 c, f). We

334 noted that, this overestimation area coincides with the excessive values of R1mm index

335 (Fig.2c, f). The strongest overestimation was found over the Guinea coast, reaching 59.21 and

336 60.51 days (resp. for JJAS 2003 and JJAS 2004, Table 2).

337 Figure 8 (second panel) is the same as Fig.2 (second panel), but displays changes in CWD

338 index. As for R1mm index, over the central Sahel, the impact was linear, the dry (wet)

339 experiments decrease (increase) CWD index for both JJAS 2003 and JJAS 2004. This result

340 confirms the strong soil moisture impact over the transition zones with a climate between dry

341 and wet regimes (Zhang et al., 2011; Koster et al., 2006). However, over Guinea and the west

342 Sahel, the changes were not linear, both dry and wet experiments lead to cause an increase, in

343 JJAS 2003 and JJAS 2004 (Fig. 8B, c).

344 Figure 9, as in Fig.3, but shows the PDF distribution of changes in CWD index. The linear

345 impacts were observed over the central Sahel for both JJAS 2003 and JJAS 2004, and over

346 west Sahel only in JJAS 2004 (Table 4). The strongest increase (decrease) on CWD index was

347 found over central Sahel with maximum change reaching 15.58 (-4.48) days in wet (dry)

348 experiments in JJAS 2004.

349 Summarizing the results of this section, as in R1mm and CDD indices, the CWD index was

350 linear over the central Sahel for both JJAS 2003 and JJAS 2004, and over the west Sahel in

351 JJAS 2004, that is, the dry (wet) experiments decrease (increase) the CWD index. The model

352 RegCM4 overestimates the duration of wet days over most of studied domains. This

353   overestimation is linked with an excessive number of wet days as documented by Diaconescu

354   et al. (2014).

355

356   **3.1.5 Maximum one-day precipitation accumulation (RX1day index).**

357   The maximum one-day precipitation accumulation (RX1day index) during JJAS 2003 and

358   JJAS 2004 is assessed in this section. Figure 10 (first panel) shows the spatial distribution of

359   the RX1day index. The observation datasets TRMM (Fig. 10b, e) and CHIRPS (Fig. 10 a, d)

360   present notable differences in terms of the spatial extent of the maximum values of the

361   RX1day index, although their large-scale pattern was similar with PCC of more than 0.84 for

362   both JJAS 2003 and JJAS 2004 (Table 2). Over the Guinea and Sahel regions, the spatial

363   extent of RX1day index maximum values more than 80 mm was large in the TRMM datasets,

364   while CHIRPS datasets showed it confined over the coastline of the Gulf of Guinea. TRMM

365   observations overestimated the RX1day index over the most of studied domains. The largest

366   RX1day index was found over the central Sahel, with MB reaching 35.78 and 31.66 (for JJAS

367   2003 and JJAS 2004, respectively; Table 2).

368   The control experiments captured the spatial pattern with PCC values of 0.50 and 0.4 (JJAS

369   2003 and JJAS 2004, respectively; Table 2). This low coefficient of PCC was also obtained

370   by Thanh et al. (2017) over Asia with RegCM4 (correlation < 0.3). The model simulations

371   failed to capture the magnitude and spatial extent of the RX1day index maxima values. The

372   control experiments underestimated the RX1day index over most of studied domains. The

373   RX1day index was underestimated throughout studied domains; this was also due to the

374   excessive light precipitation, simulated by the current physical parameterization of RegCM4.

375   The largest underestimation was located over the Guinea coast and the west Sahel. For

376   instance, over the west Sahel, the MB was approximately -38.07 and -36.67 mm (JJAS 2003

377   and JJAS 2004, respectively; Table 2).

378   Figure 10 (second panel) is similar to Fig. 2 (second panel), but displays changes in the

379   RX1day index. For the SDII, the impact of initial soil moisture anomalies on the RX1day

380   index was not linear, and a similar mixture of increase and decrease in RX1day index is

381   shown for dry and wet experiments over most of the studied domains (Fig. 10, second panel).

382   Figure 11 is similar to Fig. 3, but shows the PDF distribution of changes in the RX1day index.

383   The impact on RX1day index increase for both dry and wet experiments and was found over

384   most of studied domains (Fig.11). The strongest increase in RX1day index was observed over

385   Guinea in wet experiments 26.14 and 14.93 for JJAS 2003 and JJAS 2004, respectively.

386 In summary, RegCM4 underestimates the maximum one-day precipitation accumulation over

387 most of studied domains. The impact on RX1day index increase for both dry and wet

388 experiments and was found over most of studied domains.

389

3.1.6 Precipitation percent due to very heavy precipitation days (R95pTOT index)

391 In this section, we investigated the precipitation percentage due to very heavy precipitation

392 days during JJAS 2003 and JJAS 2004. Figure 12 (first panel) is the same as Fig. 2 (first

393 panel), but shows the spatial distribution of the R95pTOT index. TRMM (Fig. 12b, e) and

394 CHIRPS observations (Fig. 12a, d) presented a similar spatial pattern over the entire West

395 African domain, with a PCC value of 0.91 for both JJAS 2003 and JJAS 2004 (Table 2).

396 However, some biases in spatial extent were noticed for R95pTOT index maxima. TRMM

397 observation extended the maximum R95pTOT index over the Guinea and Sahel regions (Fig.

398 10, first panel), while CHIRPS confined them over the Guinea coast. Overall, TRMM showed

399 a dominant overestimation compared to CHIRPS over the West African domain by

400 approximately 16.54% and 18.54 % (JJAS 2003 and JJAS 2004, respectively; Table 2). The

401 control experiments (Fig. 12c, f) capture the spatial pattern with PCC values of 0.59 and 0.55

402 (JJAS 2003 and JJAS 2004, respectively; Table 2). As with SDII and RX1day indices, the

403 control experiments underestimated the values of the R95pTOT index, while they

404 overestimated the R1mm index. This was also due to the current physical parameterisation

405 scheme of the RegCM4 model, which results in a positive bias for the number of wet days

406 with a low precipitation threshold (e. g., 1 mm•day-1), and a negative bias for the indices of

407 the number of wet days with a higher precipitation threshold (e.g., 10 mm•day-1, not shown

408 here).

409 The control experiments underestimated the R95pTOT index over the different studied

410 domains. The largest underestimation of the R95pTOT index was located over the Guinea

411 coast with MB more than −43.22 and −46.61 % (for JJAS 2003 and JJAS 2004, respectively;

412 Table 2).

413 Figure 12 (second panel) is similar to Fig. 2 (second panel), but displays changes in the

414 R95pTOT index. Both dry and wet experiments tended to cause an increase in the R95pTOT

415 index over the orographic regions. Therefore, the initial soil moisture conditions, whether dry

416 or wet, tended to reinforce extreme floods.

417 Figure 13 is the same as Fig. 3 but shows the PDF distribution of changes in the R95pTOT

418 index indicating an increase in the R95pTOT index for both wet and dry experiments over

419   most of the studied domains. The strongest increase in R95pTOT index was found over the

420   west Sahel and Guinea coast with maximum change values around 4.03% (JJAS 2004) and

421   4.33% (JJAS 2003), respectively (Table 4).

422   In summary, RegCM4 underestimates the precipitation percentage due to very heavy

423   precipitation days over the West African domain. The initial soil moisture conditions, whether

424   dry or wet, accentuate the precipitation percent due to very heavy precipitation days. This

425   result is consistent with Liu et al.'s (2014) work over Asia using RegCM4. The impact on

426   R95pTOT index led to an increase in wet and dry experiments over most of the studied

427   domains.

428

429   **3.2. Seasonal temperature extreme indices**

430   In this section, using daily maximum and minimum temperatures, we analyze four extreme

431   temperature indices (Table 1) in RegCM4 simulations over West Africa. All temperature

432   indices were calculated for JJAS 2003 and JJAS 2004. Table 3 summarizes the PCC and MB

433   of all temperature indices studied in this section for EIN reanalysis and model simulations

434   derived from control experiments with initial soil moisture from ERA20C reanalysis, with

435   respect to GTS observations, calculated over the domains presented in Fig. 1, during the JJAS

436   2003 and JJAS 2004.

437

438   **3.2.1. Maximum value of daily maximum temperature (TXx index)**

439   In this section, we analyze the TXx index, which gives the hottest day's temperature during

440   JJAS 2003 and JJAS 2004. Figure 14 (first panel) shows the TXx index (in °C) from GTS

441   observations (Fig. 14a, d) and EIN reanalysis (Fig. 14b, e) for JJAS 2003 and JJAS 2004 and

442   their corresponding simulated control experiments (Fig. 14c, f) with the initial soil moisture

443   of the reanalysis ERA20C. The GTS observation showed the highest values of the TXx index

444   observed over the Sahara, at more than 46 °C. The lowest values (less than 32 °C) were found

445   over the Guinea coast (Fig. 14a, d). Fan Y. and Huug van den Dool (2008) in their work

446   showed that the Reanalysis 2 m temperature data sets may not be suitable for model forcing

447   and validation. We have chosen NOAA-CPC GTS observation dataset as reference in this

448   study over ERA-Interim reanalysis, because NOAA-CPC GTS consists of a blending of

449   satellite-based data collection and in situ data archive available in the GTS (Global

450   Telecommunication System). The EIN reanalysis has similar large-scale patterns with a PCC

value of 0.99 over the entire West African domain (Table 3). However, some local biases are shown for magnitude and spatial extent of these maxima and minima. The reanalysis of the EIN (Fig. 14b, e) shows lower values (less than 28 °C) of the TXx index over a large area along the Guinea coastline compared to GTS datasets. Conversely, GTS observation presented higher values of the TXx index (up to 48 °C) over a large area compared to the EIN reanalysis (Fig.14a, d), which showed a negative bias of the TXx index over most of the studied domains (Table 3).

The control experiments (Fig. 14c, f) reasonably replicate the large-scale patterns of the TXx index values with PCCs up to 0.99 (Table3) over the entire West African domain; however, they exhibited some biases at a local scale. The control experiments were closer to the maximum and minimum values displayed in the GTS observation. The control simulations overestimated the TXx values over the central and west Sahel, and over the Guinea coast (Table 3). The greatest overestimation was found over the west Sahel with MB of approximately 3.02 and 2.02 °C (for JJAS 2003 and JJAS 2004, respectively; Table 3). However, the biases obtained for the TXx index in this study were much lower than those obtained by Thanh et al. (2017), who used RegCM4 over Asia where it reached 8 °C.

Figure 14 (second panel) displays changes in the TXx index for JJAS 2003 and JJAS 2004 for dry (Fig. 14g, i for JJAS 2003 and JJAS 2004, respectively) and wet experiments (Fig. 14h, j for JJAS 2003 and JJAS 2004, respectively) with respect to their corresponding control experiments; the dotted area shows changes with a statistical significance of 10%. The impact of the initial soil moisture conditions on the TXx index was linear over most of studied domains; that is, the dry experiments led to an increase in the TXx index values, while the wet experiments favoured a decrease in the TXx index values.

The PDF distributions of TXx index changes for JJAS 2003 and JJAS 2004 over (a) the central Sahel, (b) West Sahel, (c) Guinea, and (d) West Africa derived from dry and wet experiments compared to the corresponding control experiments are shown in Fig. 15. Table 5 summarizes the maximum values of changes obtained on the PDF's for extreme temperature indices used in this study. As mentioned above, the results confirmed the linear impact on the TXx index over most of studied domains (Fig. 15). The strongest decrease (increase) in the TXx index was found over the central Sahel with a maximum change values around −2.57 °C (more than 1.69 °C) in wet (dry) experiments in JJAS 2004.

482 In summarizing this section, during JJAS 2003 and 2004, the RegCM4 model overestimates
483 and underestimates the hottest day's temperature over the Sahel (west and central) and Guinea
484 coast. The impact on the TXx index is linear over most of studied domains; that is, the dry
485 (wet) experiments decrease (increase) the TXx index.

486

3.2.2. Minimum value of daily maximum temperature (TXn index).

488 In this section, we investigated the TXn index which gives the lowest day's temperature
489 during JJAS 2003 and JJAS 2004. Figure 16 (first panel) is the same as Fig.14 (first panel)
490 but presents the spatial distribution of the TXn index. GTS observation (Fig.16a, d) and EIN
491 reanalysis (Fig.16b, e) display similar features with PCC reached 0.99 (for JJAS 2003 and
492 JJAS 2004, Table 3). The maxima and minima values of TXn index were located over the
493 Sahara and the Guinea coast respectively. However, there were some differences at the local
494 scale in terms of spatial extent and magnitude. The EIN reanalysis presented a larger spatial
495 extent of the maxima (greater than 36°C) and minima (less than 24°C) compared to GTS
496 observation. Generally, the EIN reanalysis showed a negative bias value over most of the
497 studied domains (for both JJAS 2003 and JJAS 2004 Table3. The strongest negative bias was
498 found over the west Sahel with MB of approximately -1.48 and -1.73°C (resp. for JJAS 2003
499 and JJAS 2004, Table 3).

500 The control experiments showed a good agreement with the GTS datasets in the large scale
501 patterns with PCC of approximately 0.99, however, the magnitude of the TXn index over
502 most of studied domains was overestimated. The strongest positive bias was observed over
503 west Sahel domain, the MB of approximately 6.56 and 5.44 °C (resp. JJAS 2003 and JJAS
504 2004, Table 3). The biases obtained in this study were lower than those of a similar study
505 carried out by Thanh et al. (2017) over Asia using RegCM4.

506 As for Fig.14 (second panel), the Figure 16 (second panel) displayed changes in TXn index.
507 The impact on TXn index of the initial soil moisture anomalies was linear over most of
508 studied domains, that is, the dry experiments led to an increase of TXn index values while the
509 wet experiments favor a decrease of TXn index values.

510 Figure 16 (second panel) is similar to Fig.14 (second panel) but displays the PDF distribution
511 of changes in TXn index. The impact on TXn index was linear over most of the domain
512 studied, although this impact is rather weak as compared to the TXx index. The strongest
513 increase (decrease) in TXn index are found over the central (west) Sahel reaching 1.03 °C (-
514 1.67°C) in dry (wet) experiments, in JJAS 2004 (JJAS 2004) (Table5).

515 In summary, RegCM4 overestimated the lowest day's temperature during JJAS 2003 and
516 JJAS 2004 over the whole West African domain. As for TXx index, the impact on TXn index
517 to soil moisture anomalies was linear over most of studied domains, that is, dry (wet)
518 experiments cause an increase (decrease) of TXn index values.

519

3.2.3. Minimum value of daily minimum temperature (TNn index).

521 In this section, we examine the TNn index, which gives the lowest temperature at night during
522 JJAS 2003 and JJAS 2004. Figure 18 (first panel) is the same as Fig. 14 (first panel) but
523 displays the spatial distribution of the TNn index. GTS observations (Fig. 18 a, d) show the
524 maxima of TNn index values above 15° N latitude, not exceeding 27 °C, while the minima
525 values are less than 17 °C and are located over the mountainous regions such as the Cameroon
526 Mountains, Jos Plateau, and Guinea Highlands. The EIN reanalysis showed a similar spatial
527 pattern as GTS observation, with a PCC value of approximately 0.99 over the entire West
528 African domain (Table 3) despite some biases at the local scale. The EIN reanalysis (Fig. 18
529 b, e) displayed the highest value of the TNn index (exceeding 27 °C) compared to GTS
530 observation, and were located over a large area above 15° N. The EIN reanalysis also showed
531 the lowest values (less than 21 °C) of the TNn index compared to the GTS observation,
532 located over the orographic regions. The EIN reanalysis overestimated the TNn index values
533 over most of the studied domains. The strongest positive bias was observed over the west
534 Sahel, the MB reached 3.43 and 2.98 °C for JJAS 2003 and JJAS 2004, respectively (Table
535 3).

536 The control experiments (Fig. 18 c, f) showed good agreement with GTS observations with
537 PCC values of approximately 0.99; however, they exhibited some biases at the local scale.
538 The control experiments overestimated the magnitude of the TNn index over most of studied
539 domains.

540 The strongest positive bias was observed over the west Sahel, the MB was approximately 3.30
541 °C and 2.55 °C for JJAS 2003 and JJAS 2004, respectively (Table 3). These positive biases
542 obtained in simulating the TXx, TXn, and TNn indices were opposite to the cold bias known
543 from RegCM4 in mean climate simulation (Koné et al., 2018, Klutse et al., 2016). It is
544 difficult to determine the origin of RegCM4 temperature biases, as they can depend on several
545 factors, such as surface energy fluxes and water, cloudiness, and surface albedo (Sylla et al.,
546 2012; Tadross et al., 2006).

547 Figure 18 (second panel) is the same as Fig. 14 (second panel), but displays changes in the

548 TNn index. Over the central and west Sahel, both dry and wet experiments led to a decrease.

549 Conversely, over the Guinea coast, we found an increase.

550 Figure 19 is the same as Fig. 15 but shows the PDF distribution of changes in the TNn index.

551 A linear impact was found over west Sahel and Guinea coast only in JJAS 2004, that is, wet

552 (dry) experiments increase (decrease) the TNN index (Fig.19; Table 5). The strongest increase

553 (decrease) in TNn index in wet (dry) experiment was found over Guinea coast (west Sahel),

554 with maximum change values around 0.11 °C and (−1.15 °C) in JJAS 2004 (JJAS 2003)

555 (Table 5).

556 In summary, RegCM4 overestimated the lowest temperature at night during JJAS 2003 and

557 JJAS 2004 over the different studied domains. A linear impact was found over west Sahel and

558 Guinea coast only in JJAS 2004, that is, wet (dry) experiments increase (decrease) the TNN

559 index

560 **3.2.4. Maximum value of daily minimum temperature (TNx index)**

561 In this section, we turned our attention to TNx index, which gives the warmest night

562 temperature during JJAS 2003 and JJAS 2004. Figure 20 (first panel) is the same as Fig. 14

563 (first panel), but for the TNx index. GTS observations (Fig. 20 a, d) showed that the maxima

564 of the TNx index values over the Sahara reached 40 °C, while the minima around 24 °C were

565 located over the Guinea coast sub-region. The EIN reanalysis (Fig. 20b, e) showed similar

566 large-scale patterns with PCC values of 0.99, but some biases can be noticed between the

567 GTS and EIN datasets. The EIN reanalysis underestimated the maxima (not exceeding 38 °C)

568 and minima (less than 22 °C) located over the Sahara and the orographic regions such as the

569 Cameroon Mountains, Jos Plateau, and Guinea Highlands. The EIN reanalysis displayed

570 negative MB over the Guinea coast with MB approximately −3.11 °C and −3.14 °C (JJAS

571 2003 and JJAS 2004, respectively; Table 3).

572 The control experiments (Fig. 20c, f) successfully reproduced the general features of the TNx

573 index with a PCC value of 0.99, but some differences were shown at the local scale. Unlike

574 the TNn index, the control experiments underestimated the TNx index over most of the

575 studied domains. The strongest negative bias was found over the central Sahel, MB was

576 approximately −3.35 °C and −3.32 °C (for JJAS 2003 and JJAS 2004, respectively; Table 3).

577 This underestimation of the TNx index seems to be systematically related to the cold bias in

578 RegCM4 over West Africa, which has been reported in several papers (Koné et al., 2018,

579 Klutse et al., 2016).

580   Figure 20 (second panel) is the same as Fig. 14 (second panel) but displays changes in the

581   TNx index. Like for the TNn index, the impact on the TNx index of initial soil moisture

582   conditions was somewhat linear over the central Sahel, and dry experiments led to an increase

583   in the TNx index values, while the wet experiments favoured a decrease in the TNx index

584   values. However, over the west Sahel, both wet and dry experiments led to a dominant

585   decrease. Conversely, over the Guinea coast, although the signal was weak, both dry and wet

586   experiments led to a dominant increase.

587   Figure 21 is the same as Fig. 15 but displays the PDF distributions of the changes in the TNx

588   index. Like for the TNn index, the impact on the TNx index changes was linear over the

589   central Sahel. The strongest increase (decrease) in TNx index was found over the central

590   Sahel in dry (wet) experiments with maximum change approximately 0.25 (-1.67 °C) in JJAS

591   2003 (JJAS 2004) (Table 5).

592   In summary, RegCM4 underestimates the warmest night temperature during JJAS 2003 and

593   JJAS 2004 over most of studied domains. The impact on the TNx index of initial soil

594   moisture conditions was linear over the central Sahel, that is, dry (wet) experiments led to an

595   increase (decrease) in the TNx index values.

596

4. Conclusions

598   The impact on the subsequent summer extreme climate of the initial soil moisture conditions

599   over West Africa was investigated using the RegCM4-CLM45. In addition, the performance

600   of RegCM4-CLM4.5 in representing six extreme indices of precipitation and four extreme

601   indices of temperature over West Africa was also evaluated. Results have been presented for

602   JJAS 2003 (wet year) and JJAS 2004 (dry year). We performed sensitivity studies over the

603   West African domain, with a spatial resolution of 25 km. We initialized the control runs using

604   ERA20C reanalysis soil moisture, at its maximum and minimum values over the West Africa

605   domain, respectively, for dry and wet experiments.

606   Compared to the extreme indices of the observation datasets, the model overestimated and

607   underestimated the number of wet days for a low (1 mm.day^{-1}) and high threshold rain rate

608   (e.g., 10 mm.day^{-1}, not shown here). RegCM4 also underestimated the simple precipitation

609   intensity index (SDII), the maximum 1-day precipitation (Rx1day index), and the

610   precipitation percentage due to very heavy precipitation days (R95pTOT index). The current

611   physical parameterization scheme of the RegCM4 model used in our study results in a

positive bias for the number of wet days with a low precipitation threshold (e. g. 1 mm•day-1), while in a negative bias for a higher precipitation threshold (e.g. 10 mm•day-1, not shown here). However, RegCM4 generally overestimated the maximum number of CWD and CDD over the West African domain studied. The temperature extreme indices used in this study (TXx, TXn, and TNn) were also overestimated, except the TNx index, which was underestimated over most of studied domains.

The impact on extreme precipitation indices of the initial soil moisture conditions was linear only for indices related over the central Sahel to the number of precipitation events (R1mm, CDD, and CWD indices) and not for those related to the amount of precipitation (SDII, RX1day, and R95pTOT). The dry and wet experiments accentuated the precipitation percentage due to very heavy precipitation days and maximum one-day precipitation accumulation (R95pTOT and RX1day indices, respectively) over most of the studied domains.

The initial soil moisture conditions unequally affected the daily maximum and minimum temperatures over the West African domain. There was a greater impact on daily maximum temperature extremes than on the daily minimum temperature extremes. These results are consistent with those of previous studies (Jaeger and Seneviratne, 2011; Zhang et al., 2009).

The wet (dry) experiments resulted in an increase (decrease) in the TXx and TXn indices over most of the studied. The impact of initial soil moisture conditions on the indices related to the minimum temperature (TNx and TNn indices) was linear only for TNx index over central Sahel. The dry (wet) experiments cause an increase (a decrease) in the TNx.

This study helps to understand the impact of the initial soil moisture conditions on extreme events of precipitation and temperature in terms of intensity, frequency and duration over West Africa. This is a contribution to the improvement of extreme event forecasts in West Africa in highlighting the crucial role of initial soil moisture. For a proper assessment of the dependence of the model in our results, it would be appropriate to repeat the investigation using different RCMs in a multi-model framework.

Author contribution
The authors declare to have no conflict of interest with this work. B. Koné and A. Diedhiou fixed the analysis framework. B. Koné carried out all the simulations and figures production according to the outline proposed by A. Diedhiou. B. Koné and A. Diedhiou, S. Anquetin and A. Diawara worked on the analyses. All authors contributed to the drafting of this manuscript.

Acknowledgements
The research leading to this publication is co-funded by the NERC/DFID "Future Climate for Africa" programme under the AMMA-2050 project, grant number NE/M019969/1 and by IRD (Institut de Recherche pour le Développement; France) grant number UMR IGE Imputation 252RA5.

References:

Bichet, A., & Diedhiou, A. (2018a). West African Sahel has become wetter during the last 30 years, but dry spells are shorter and more frequent. Climate Research, 75(2), 155-162.

Bichet, A., & Diedhiou, A. (2018b). Less frequent and more intense rainfall along the coast of the Gulf of Guinea in West and Central Africa (1981 2014). Climate Research, 76(3), 191-201.

Danielson J.J., and Gesch D.B.: Global multi-resolution terrain elevation data 2010 (GMTED2010): U.S. Geological Survey Open-File Report 2011–1073, 26 p, 2011.

Didi Sacré Regis M , Mouhamed, L., Kouakou, K., Adeline, B., Arona, D., Koffi Claude A, K., ... & Issiaka, S. (2020). Using the CHIRPS Dataset to Investigate Historical Changes in Precipitation Extremes in West Africa. Climate, 8(7), 84.

Dee D. P., Uppala S. M., Simmons A. J., Berrisford P., Poli P., Kobayashi S., Andrae U., Balmaseda, M. A., Balsamo G., Bauer, P., Bechtold P., Beljaars A. C. M., van de Berg L., Bidlot J., Bormann N., Delsol C., Dragani R., Fuentes M., Geer A. J., Haimberger L., Healy

672 S. B., Hersbach H., Hólm E. V., Isaksen L., Kållberg P., Köhler M., Matricardi M., McNally

673 A. P., Monge-Sanz B. M., Morcrette J.-J., Park, B.-K., Peubey C., de Rosnay P., Tavolat C.,

674 Thépaut J.-N. and Vitart F.: The ERA-Interim reanalysis: configuration and performance of

675 the data assimilation system, Q. J. Roy. Meteorol. Soc., 137, 553-597,

676 https://doi.org/10.1002/qj.828, 2011.

677

678 Diaconescu E. P., Gachon P. , Scinocca J., and LapriseR.: Evaluation of daily precipitation

679 statistics and monsoon onset/retreat over west Sahel in multiple data sets. Climate Dyn., 45,

680 1325–1354, doi:10.1007/s00382-014-2383-2, 2015 .

681

682 Easterling, D.R., Meehl, G.A., Parmesan, C., Changnon, S.A., Karl, T.R. and Mearns, L.O.:

683 Climate Extremes: Observations, Modeling and Impacts. Science , 289, 2068-2074.

684 https://doi.org/10.1126/science.289.5487.2068, 2000.

685

686 Emanuel K. A.: A scheme for representing cumulus convection in large-scale models. Journal

687 of the Atmospheric Science 48: 2313–2335, 1991.

688

689 Fan Y., and van den Dool H. : A global monthly land surface air temperature analysis for

690 1948 -present, J. Geophys. Res. 113, D01103, doi: 10.1029/2007JD008470, 2008.

691

692 Folland C. K., Palmer T. N. , and Parker D. E.: Sahel rainfall and worldwide sea

693 temperatures, Nature, 320, 602 – 607, 1986.

694

695 Fontaine B., Janicot S. , and Moron V. : Rainfall anomaly patterns and wind field signals over

696 West Africa in August (1958 – 1989), J. Clim., 8, 1503 –1510, 1995.

697

698 Giorgi F., Coppola E., Solmon F., Mariotti L., Sylla M. B., Bi X., Elguindi N., Diro G. T.,

699 Nair V., Giuliani G., Cozzini S., Guettler I., O'Brien T., Tawfik A., Shalaby A., Zakey A. S.,

700 Steiner A., Stordal F., Sloan L., and Brankovic C. : RegCM4: model description and

701 preliminary tests over multiple CORDEX domains, Clim. Res., 52, 7–29,

702 doi.org/10.3354/cr01018, 2012.

703

704 Grell G., Dudhia J. and Stauffer D. R.: A description of the fifth generation Penn State/NCAR

705 Mesoscale Model (MM5), National Center for Atmospheric Research Tech Note NCAR/TN-

706 398+STR, NCAR, Boulder, CO, 1994.

707

708 Holtslag A., De Bruijn E., and Pan H. L. : A high resolution air mass transformation model

709 for short-range weather forecasting, Mon. Weather Rev., 118, 1561–1575, 1990.

710

711 Hong S. Y. and Pan H. L.: Impact of soil moisture anomalies on seasonal, summertime

712 circulation over North America in a regional climate model. J. Geophys. Res., 105 (D24), 29

713 625–29 634, 2000.

714

715 Huffman, G. J., Adler, R. F., Bolvin, D. T., Gu, G., Nelkin, E. J., Bowman, K. P., Hong, Y,

716 Stocker, E. F., and Wolff, D. B.: The TRMM multisatellite precipitation analysis: quasi-

717 global, multiyear, combined-sensor precipitation estimates at fine scale, J. Hydrometeorol., 8,

718 38–55, 2007.

719

720 Jaeger E. B., and Seneviratne S. I. : Impact of soil moisture-atmosphere coupling on

721 European climate extremes and trends in a regional climate model, Clim. Dyn., 36(9-10),

722 1919-1939, doi:10.1007/s00382-010-0780-8, 2011.

723

724 Kang S, Im E.-S. and Ahn J.-B.: The impact of two land-surface schemes on the

725 characteristics of summer precipitation over East Asia from the RegCM4 simulations Int. J.

726 Climatol. 34: 3986–3997, 2014.

727

728 Kim J-E., and Hong S-Y.: Impact of Soil Moisture Anomalies on Summer Rainfall over East

729 Asia: A Regional Climate Model Study, Journal of Climate. Vol. 20, 5732–5743, DOI:

730 10.1175/2006JCLI1358.1, 2006.

731

732 Kiehl J. T., Hack J. J., Bonan G. B., Boville, B. A., Briegleb B. P., Williamson D. L., and

733 Rasch P. J.: Description of the NCAR Community Climate Model (CCM3), Technical Note

734 NCAR/TN−420+STR, 152, 1996.

735

736 Koné B., Diedhiou A., N'datchoh E. T., Sylla M. B. , Giorgi F., Anquetin S., Bamba A.,
737 Diawara A., and Kobea A. T.: Sensitivity study of the regional climate model RegCM4 to
738 different convective schemes over West Africa. Earth Syst. Dynam., 9, 1261–1278.
739 https://doi.org/10.5194/esd-9-1261-2018, 2018.
740
741
742 Koster R. D., GUO Z. H., Dirmeyer P. A., Bonan G., Chan E., Cox P., Davies H., Gordon C.
743 T., Gordon C. T.,Lawrence D., Liu P., Lu C. H, Malyshev S., McAvaney B., Mitchell K,
744 Mocko D., Oki K., Oleson K., Pitman A., Sud Y. C. , Taylor C. M., 16 Verseghy D., Vasic
745 R., Xue Y., Yamada T.: The global land–atmosphere coupling experiment. Part I: Overview,
746 J. Hydrometeorol., 7(4), 590–610, doi:10.1175/JHM510.1, 2006.
747
748 Larsen J.: Record heat wave in Europe takes 35,000 lives. Earth Policy Institute, 2003.
749
750 Le Barbé L., Lebel L., and Tapsoba D.: Rainfall variability in west africa during the years
751 1950-1990. J. Climate, 15 :187–202., 2002.
752
753 Loveland TR, Reed BC, Brown JF, Ohlen DO, Zhu Z, Yang L, J. W. Merchant J. W.:
754 Development of a global land cover characteristics database and IGBP DISCover from 1km
755 AVHRR data. International Journal of Remote Sensing 21: 1303–1330, 2000.
756
757 Liu D., G. Wang R. Mei Z. Yu, and Yu M. : Impact of initial soil moisture anomalies on
758 climate mean and extremes over Asia, J. Geophys. Res. Atmos., 119, 529–545,
759 doi:10.1002/2013JD020890, 2014.
760
761 Klutse B. A. N., Sylla B. M., Diallo I., Sarr A., Dosio A.,Diedhiou A., Kamga A., Lamptey
762 B., Ali A., Gbobaniyi E. O., Owusu K., Lennard C., Hewitson B., Nikulin G.,& Panitz H.-J.,
763 Büchner M.: Daily characteristics of West African summer monsoon precipitation in
764 CORDEX simulations. Theor Appl Climatol. 123:369–386 DOI 10.1007/s00704-014-1352-3,
765 2016.
766

767 Nicholson, SE.: The nature of rainfall fluctuations in subtropical West-Africa. Mon. Wea.
768 Rev. 22109, 2191-2208, 1980.

769

770 Nicholson SE.: Land Surface processes and Sahel climate. Reviews of Geophysics. 38(1),
771 117-24139, 2000.

772

773 Nikulin G., Jones C., Samuelsson P., Giorgi F., Asrar G., Büchner M., Cerezo-Mota R.,
774 Christensen O. B., Déque M., Fernandez J., Hansler A., van Meijgaard E., Sylla M. B. and
775 Sushama L.: Precipitation climatology in an ensemble of CORDEX-Africa regional climate
776 simulations, J. Climate, 6057–6078, https://doi.org/10.1175/JCLI-D-11-00375.1, 2012.

777

778 Oleson K., Lawrence D. M., Bonan G. B., Drewniak B., Huang M., Koven C. D., Yang Z.-L.:
779 Technical description of version 4.5 of the Community Land Model (CLM) (No. NCAR/TN-
780 503+STR). doi:10.5065/D6RR1W7M, 2013.

781

782 Pal J. S., Small E. E. and Elthair E. A.: Simulation of regional scale water and energy
783 budgets: representation of subgrid cloud and precipitation processes within RegCM, J.
784 Geophys. Res., 105, 29579–29594, 2000.

785

786 Peterson T. C., Folland C., Gruza G., Hogg W. Mokssit A., Plummer N. : Report on the
787 activities of the working group on climate change detection and related rapporteurs 1998-
788 2001. Geneva (Switzerland): WMO Rep. WCDMP 47, WMO-TD 1071, 2001.

789

790 Philippon N., Mougin E. , Jarlan L. , and Frison P.-L.: Analysis of the linkages between
791 rainfall and land surface conditions in the West African monsoon through CMAP, ERS-
792 WSC,and NOAA-AVHR R data. J. Geophys. Res., 110, D24115,
793 doi:10.1029/2005JD006394, 2005.

794

795 Reynolds, R. W. and Smith, T. M.: Improved global sea surface temperature analysis using
796 optimum interpolation, J. Climate, 7, 929–948, 1994.

797

798   Simmons A. S., Uppala D. D. and Kobayashi S.: ERA-interim: new ECMWF reanalysis

799   products from 1989 onwards, ECMWF Newsl., 110, 29–35, 2007.

800   Solmon F., Giorgi F., and Liousse C.: Aerosol modeling for regional climate studies:

801   application to anthropogenic particles and evaluation over a European/African domain, Tellus

802   B, 58, 51–72, 2006.

803

804   Sundqvist H. E., Berge E., and Kristjansson J. E.: The effects of domain choice on summer

805   precipitation simulation and sensitivity in a regional climate model, J. Climate, 11, 2698–

806   2712, 1989.

807

808   Sylla MB, Giorgi F, Stordal F.: Large-scale origins of rainfall and temperature bias in high

809   resolution simulations over Southern Africa. Climate Res. 52: 193–211, DOI:

810   10.3354/cr01044, 2012.

811

812   Tadross MA, Gutowski WJ Jr, Hewitson BC, Jack C, New M.: MM5 simulations of

813   interannual change and the diurnal cycle of southern African regional climate. Theor. Appl.

814   Climatol. 86(1–4):63–80, 2006.

815

816   Thanh N.-D., Fredolin T. T., Jerasorn S., Faye C., Long T.-T., Thanh N.-X., Tan P.-V., Liew

817   J., Gemma N., Patama S., Dodo G. and Edvin A.: Performance evaluation of RegCM4 in

818   simulating extreme rainfall and temperature indices over the CORDEX-Southeast Asia

819   region. Int. J. Climatol. 37: 1634–1647. Published online 28 June 2016 in Wiley Online

820   Library (wileyonlinelibrary.com) DOI: 10.1002/joc.4803, 2017.

821

822   Uppala S., Dee D., Kobayashi S., Berrisford P. and Simmons A.: Towards a climate data

823   assimilation system: status update of ERA-interim, ECMWF Newsl., 15, 12–18, 2008.

824

825   Wang, G., Yu, M., Pal, J. S., Mei, R., Bonan, G. B., Levis, S., and Thornton, P. E.: On the

826   development of a coupled regional climate vegetation model RCM-CLM-CN-DV and its

827   validation its tropical Africa, Clim. Dynam, 46, 515–539, 2016.

828

829 You Q., Kang S., Aguilar E., Pepin N., Flügel W.-A., Yan Y. , Xu Y., Zhang Y. , and Huang
830 J. : Changes in daily climate extremes in China and their connection to the large scale
831 atmospheric circulation during 1961–2003, Clim. Dyn., 36(11-12), 2399–2417,
832 doi:10.1007/s00382-009-0735-0, 2010.

833

834 Zakey A. S., Solmon F., and Giorgi F.: Implementation and testing of a desert dust module in
835 a regional climate model, Atmos. Chem. Phys., 6, 4687–4704, https://doi.org/10.5194/acp-6-
836 4687-2006, 2006.

837

838 Zeng X., Zhao M. and Dickinson R .E.: Intercomparison of bulk aerodynamic algorithms for
839 the computation of sea surface fluxes using TOGA COARE and TAO DATA, J. Climate, 11,
840 2628-2644, 1998.

841

842 Zhang J, Wang W.C., and Wu L.: Land–atmosphere coupling and diurnal temperature range
843 over the contiguous United States. Geophys Res Lett 36:L06706.
844 doi:10.1029/2009GL037505, 2009.

845

846 Zhang J. Y., Wu L. Y. and Dong W. : Land-atmosphere coupling and summer climate
847 variability over East Asia, J. Geophys. Res., 116,D05117, doi 10.1029/2010JD014714, 2011.
848
849
850
851
852
853
854
855
856
857
858
859

TABLES AND FIGURES.

861

	Extreme indices	Definition	Units
	Extreme Rainfall Indices		
1	R1mm	Number of wet days (daily precipitation $\geq$ 1mm)	day
2	SDII	The amount of precipitation mean on wet days (daily precipitation $\geq$ 1mm)	mm.day^{-1}
3	CDD	Maximum number of consecutive dry days (daily precipitation $<$ 1 mm.day^{-1})	day
4	CWD	Maximum number of consecutive wet days (daily precipitation $\geq$ 1 mm.day^{-1})	day
5	RX1day	The maximum one-day precipitation accumulation	mm
6	R95pTOT	Precipitation percent due to very heavy precipitation days.	%
	Extreme temperature indices		
7	TXn	Minimum value of daily maximum temperature	°C
8	TXx	Maximum value of daily maximum temperature	°C
9	TNn	Minimum value of daily minimum temperature	°C
10	TNx	Maximum value of daily minimum temperature	°C

862

Table1: The 10 extreme climate indices used in this study.

864

865

866

867

		Central Sahel		West Sahel		Guinea coast		West Africa	
		MB	PCC	MB	PCC	MB	PCC	MB	PCC
R1mm	TRMM_2003	**-6.76**	0.98	-3.15	0.99	**8.89**	0.99	-1.12	**0.98**
	CTRL_2003	33.17	0.98	-5.25	0.96	**53.16**	0.96	22.18	**0.96**
	TRMM_2004	**-7.51**	0.98	-3.42	0.99	**10.44**	0.98	-1.34	**0.98**
	CTRL_2004	29.50	0.98	1.34	0.96	**55.46**	0.96	23.85	**0.95**
SDII	TRMM_2003	**2.67**	0.96	0.22	0.94	**-5.24**	0.95	1.20	**0.86**
	CTRL_2003	-7.52	0.97	-9.95	0.94	**-13.62**	0.77	-7.67	**0.73**
	TRMM_2004	**2.07**	0.96	0.45	0.96	**-6.44**	0.94	1.16	**0.86**
	CTRL_2004	-7.01	0.97	-9.37	0.94	**-14.65**	0.81	-7.59	**0.77**
CDD	TRMM_2003	1.21	0.95	0.89	0.93	-0.93	0.94	**-2.29**	**0.92**
	CTRL_2003	0.93	0.90	**14.49**	0.91	**-7.84**	0.66	**2.63**	**0.85**
	TRMM_2004	2	0.95	1.58	096	-3.17	0.92	**-1.75**	**0.94**
	CTRL_2004	4.75	0.91	**17.51**	0.95	**-9.43**	0.68	**6.99**	**0.89**
CWD	TRMM_2003	**-0.48**	0.92	0.80	0.94	**2.47**	0.92	0.37	**0.90**
	CTRL_2003	45.56	0.83	18.44	0.75	**59.21**	0.88	31.20	**0.81**
	TRMM_2004	**-0.68**	0.92	0.97	0.92	**2.38**	0.89	0.26	**0.87**
	CTRL_2004	36.78	0.79	20.48	0.78	**60.51**	0.82	29.74	**0.79**
RX1day	TRMM_2003	**35.78**	0.92	25.31	0.89	14.31	0.86	26.02	**0.84**
	CTRL_2003	-26.46	0.78	**-38.07**	0.91	**-30.28**	0.54	-20.08	**0.50**
	TRMM_2004	**31.66**	0.91	20.19	0.91	10	0.88	22.19	**0.85**
	CTRL_2004	-22.89	0.46	**-36.67**	0.88	**-42.44**	0.42	-20.23	**0.40**
R95pTOT	TRMM_2003	23.19	0.92	13.31	0.94	-0.23	0.96	**16.54**	**0.91**
	CTRL_2003	-27.67	0.67	-33.39	0.77	**-43.22**	0.65	-29.12	**0.59**
	TRMM_2004	23.26	0.91	12.32	0.94	-0.93	0.95	**18.54**	**0.91**
	CTRL_2004	-24.38	0.46	-31.75	0.80	**-46.61**	0.60	-27.45	**0.55**

869

870 **Table 2**: The pattern correlation coefficient (PCC) and the mean bias (MB) of R1mm (in
871 day), SDII (in mm.day-1), CDD (in day), CWD (in day), RX1day (in mm) and R95pTOT (in
872 %) indices for TRMM observation and their corresponding control experiments (initialized
873 with initial soil moisture of ERA20C reanalysis) with respect to CHIRPS, calculated over
874 Guinea coast, central Sahel, west Sahel and the entire West African domain for JJAS 2003
875 and JJAS 2004.

876

877

		Central Sahel		West Sahel		guinea		West Africa	
		MB	PCC	MB	PCC	MB	PCC	MB	PCC
TXx	EIN_2003	**-2.17**	0.99	**-3.05**	0.99	**-4**	0.99	**-2.77**	**0.99**
	CTRL_2003	2.10	0.99	**3.02**	0.99	-1.34	0.99	0.32	**0.99**
	EIN_2004	**-2.44**	0.99	**-3.86**	0.99	**-3.84**	0.99	**-2.94**	**0.99**
	CTRL_2004	1.14	0.99	**2.02**	0.99	-1.41	0.99	-0.16	**0.99**
TXn	EIN_2003	0.31	0.99	**-1.48**	0.99	-0.70	0.99	0.50	**0.99**
	CTRL_2003	5.12	0.99	**6.56**	0.99	3.76	0.99	**5.65**	**0.99**
	EIN_2004	-0.76	0.99	**-1.73**	0.99	-1.38	0.99	-0.32	**0.99**
	CTRL_2004	3.43	0.99	**5.44**	0.99	2.75	0.99	**4.14**	**0.99**
TNn	EIN_2003	3.08	0.99	**3.43**	0.99	1.28	0.99	3.15	**0.99**
	CTRL_2003	2.37	0.99	**3.30**	0.99	1.53	0.99	1.45	**0.99**
	EIN_2004	3.28	0.99	**2.98**	0.99	1.20	0.99	3.11	**0.99**
	CTRL_2004	2.09	0.99	**2.55**	0.99	1.28	0.99	0.71	**0.99**
TNx	EIN_2003	-0.69	0.99	-1.79	0.99	**-3.11**	0.99	-1.62	**0.99**
	CTRL_2003	-1.91	0.99	-2.86	0.99	**-3.35**	0.99	-3.85	**0.99**
	EIN_2004	-0.82	0.99	-1.43	0.99	**-3.14**	0.99	-1.71	**0.99**
	CTRL_2004	-1.90	0.99	-2.54	0.99	**-3.32**	0.99	-3.99	**0.99**

878

879 **Table 3**: The pattern correlation coefficient (PCC) and the mean bias (MB in°C) of TXx,

880 TXn, TNn and TNx indices from the EIN reanalysis and their corresponding control

881 experiments (initialized with initial soil moisture of ERA20C reanalysis) with respect to GTS,

882 calculated for Guinea coast, central Sahel, west Sahel and the entire West African domain for

883 JJAS 2003 and JJAS 2004.

884

885

Precipitation indices		Central Sahel		West Sahel		Guinea coast		West Africa	
		ΔWC	ΔDC	ΔWC	ΔDC	ΔWC	ΔDC	ΔWC	ΔDC
R1mm (day)	2003	8.14	**-5.19**	**12.02**	0.69	3.92	2.88	4.67	1.75
	2004	10.01	-3.79	10.14	0.56	4.90	3.57	7.90	2.61
SDII (mm/day)	2003	0.07	0.11	-0.11	0.14	0.70	0.17	0.29	0.31
	2004	0.03	0.09	0.26	-0.07	0.56	0.22	0.24	0.21
CWD (day)	2003	13.25	-3.15	6.61	0.64	12.24	4.05	9.43	1.09
	2004	**15.58**	**-4.48**	7.20	-0.19	6.08	3.18	11.89	-0.37
CDD (day)	2003	-2.80	2.58	**-12.73**	0.83	-0.68	-1.31	-1.53	0.19
	2004	-5.92	**3.80**	-7.75	2.75	-0.93	-1.46	-3.57	-0.44
RX1day (mm)	2003	1.97	3.78	0.11	0.65	**26.14**	4.17	7.16	7.27
	2004	3.35	3.03	7.05	0.19	**14.93**	15.73	6.46	2.28
R95pTOT (%)	2003	1.54	1.77	2.88	1.53	**4.33**	2.37	2.83	2.46
	2004	1.66	0.89	**4.03**	0.43	1.69	0.92	1.37	2.43

886

887 **Table 4:** Summary Table of maximum values of change on PDF's for R1mm, SDII, CDD,
888 CWD, RX-1day and R95pTOT indices.

889

890

891

892

893

894

895

896

897

898

899

900

901

902

903

904

905

Temperature indices		Central Sahel		West Sahel		Guinea coast		West Africa	
		ΔWC	ΔDC	ΔWC	ΔDC	ΔWC	ΔDC	ΔWC	ΔDC
TXx	2003	-2.54	1.14	-2.11	0.90	-0.34	0.68	-0.89	1.06
	2004	**-2.57**	**1.69**	-1.58	0.98	-0.32	1.01	-0.86	1.27
TXn	2003	-1.37	0.81	**-1.67**	-0.05	-0.06	0.28	-0.50	0.59
	2004	-1.09	**1.03**	-0.93	0.55	-0.04	0.31	-0.38	0.61
TNn	2003	-0.37	-0.20	-0.23	**-1.15**	0.05	0.04	-0.20	0.03
	2004	-0.03	-0.37	0.06	-1.07	**0.11**	-0.03	-0.05	-0.11
TNx	2003	-1.29	**0.25**	-0.94	-1.37	0.12	0.04	-0.49	0.13
	2004	**-1.67**	0.15	-0.62	-1.13	0.02	0.03	-0.51	-0.07

906

907 **Table 5:** Summary Table of maximum values of change on PDF's for TXx, TXn, TNn and
908 TNx indices.

909

910

911

912

913

914

915

916

917

918

919

920

921

922

923

Figure 1: Topography of the West African domain. The analysis of the model result has an emphasis on the whole West African domain and the three subregions Guinea coast, central Sahel and west Sahel, which are marked with black boxes.
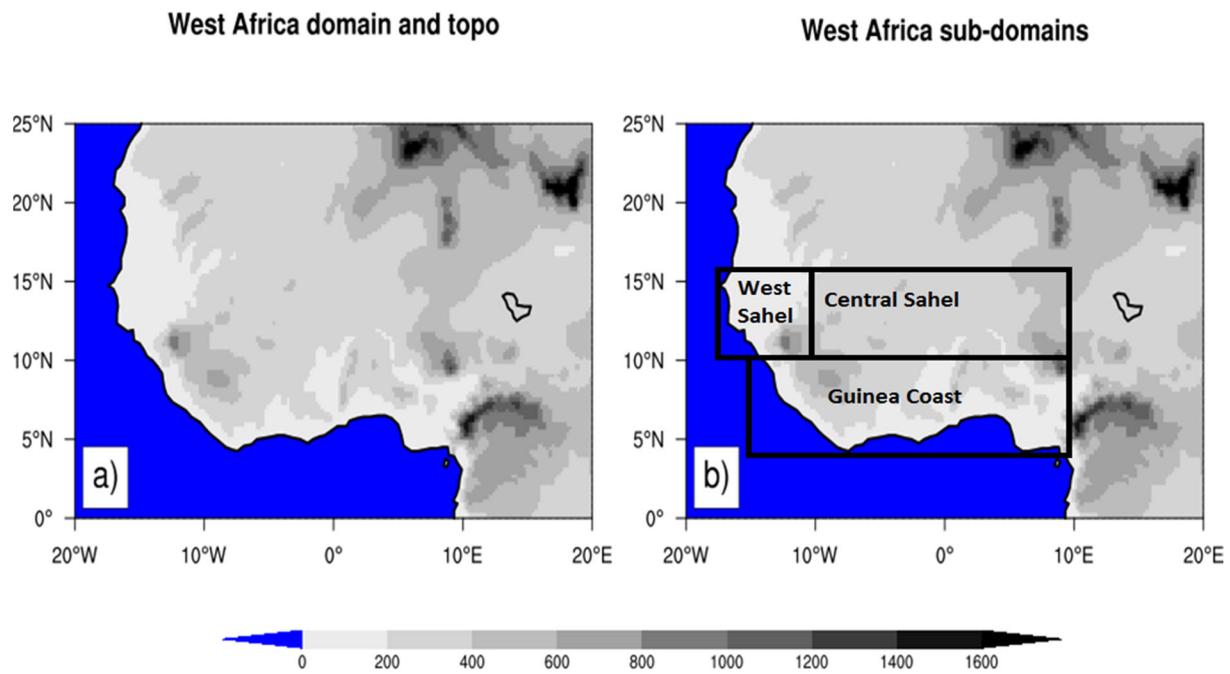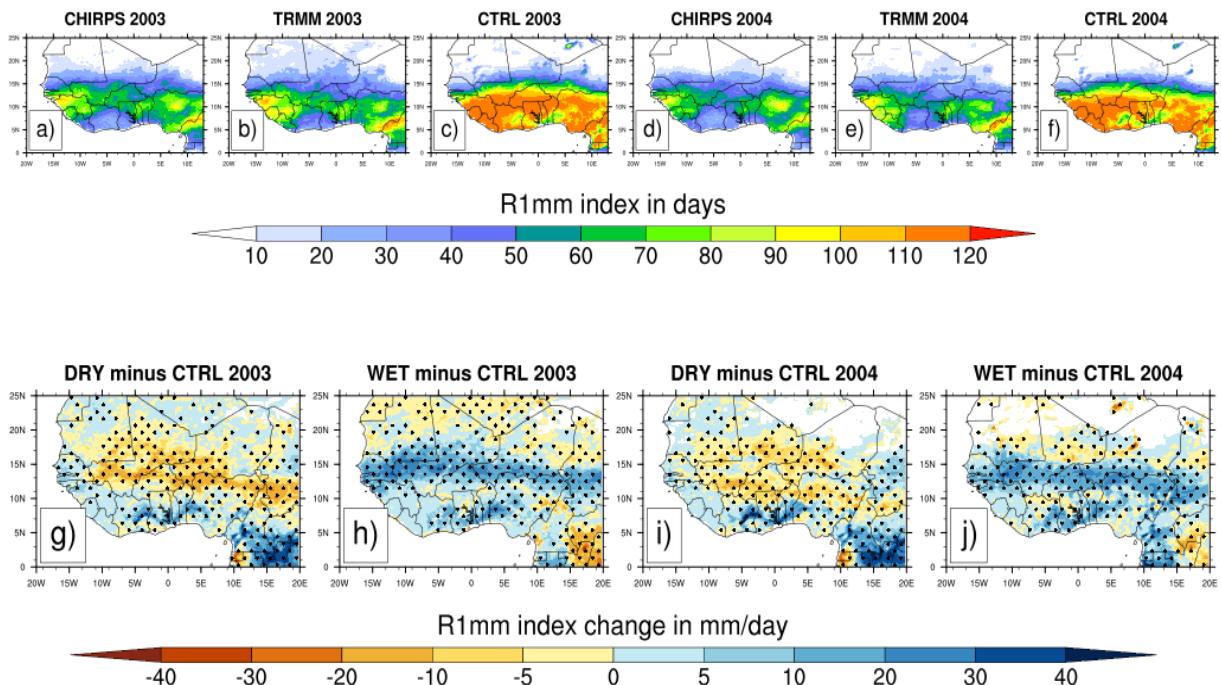
Figure2: Mean values of the number of the wet days (R1mm index in days) from CHIRPS (a and d) and TRMM(b and e) observations for JJAS 2003 and JJAS 2004 and their corresponding simulated control (CTRL) experiments (c and f) initialized with initial soil moisture of the reanalysis of ERA20C (first panel) and changes in R1mm index in days (second panel) for JJAS 2003 and JJAS 2004, from dry (g and i) and wet (h and j) experiments with respect to the corresponding control experiments. Areas with values passing the 10% significance test are dotted.
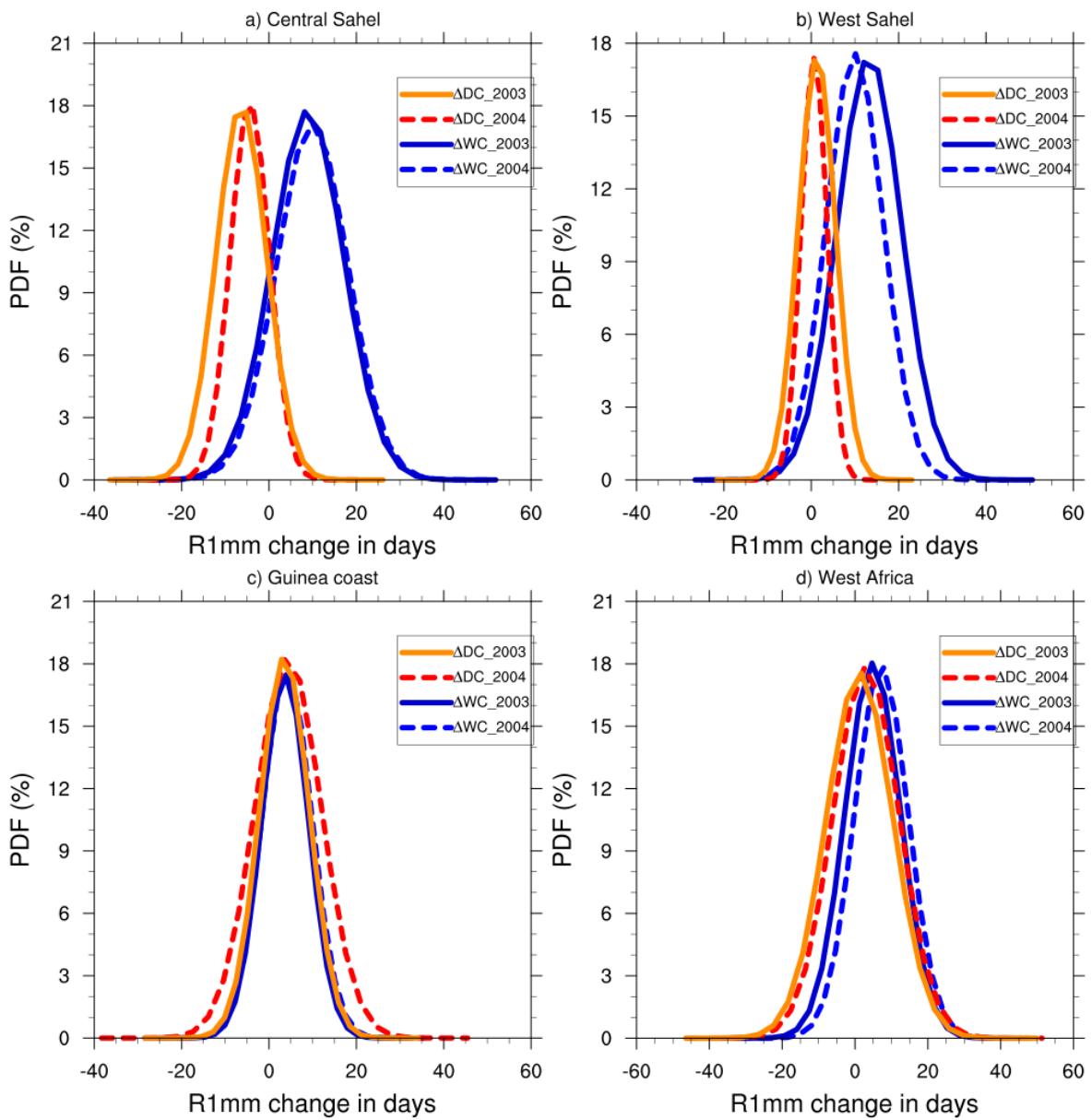
966
967

968   **Figure3:** PDF distributions (%) of mean values of the number of the wet days change in JJAS
969   2003 and JJAS 2004, over (a) central Sahel , (b) West Sahel, (c) Guinea and (d) West Africa
970   derived from dry (ΔDC) and wet (ΔWC) experiments with respect to their corresponding
971   control experiment.

972
973
974
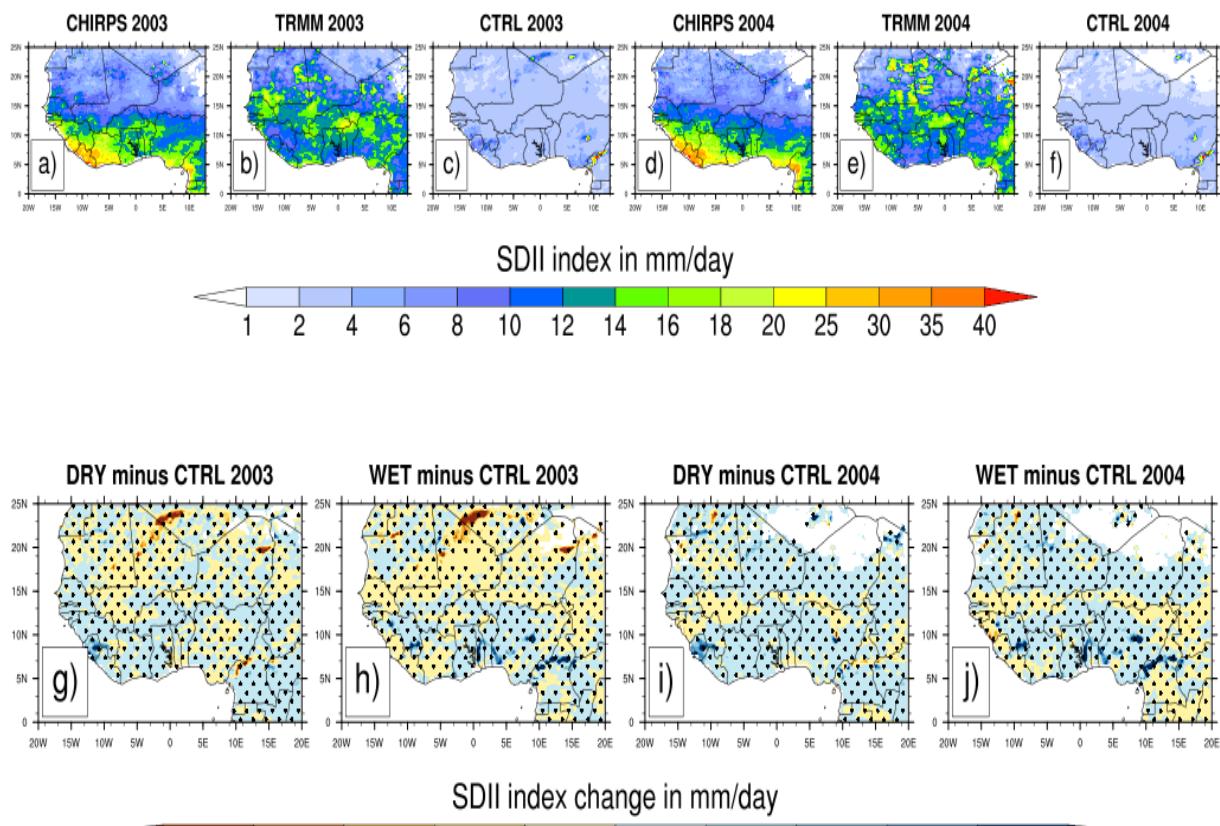
Figure4: Same as Fig. 2 but for the SDII index (in mm.day^{-1}).
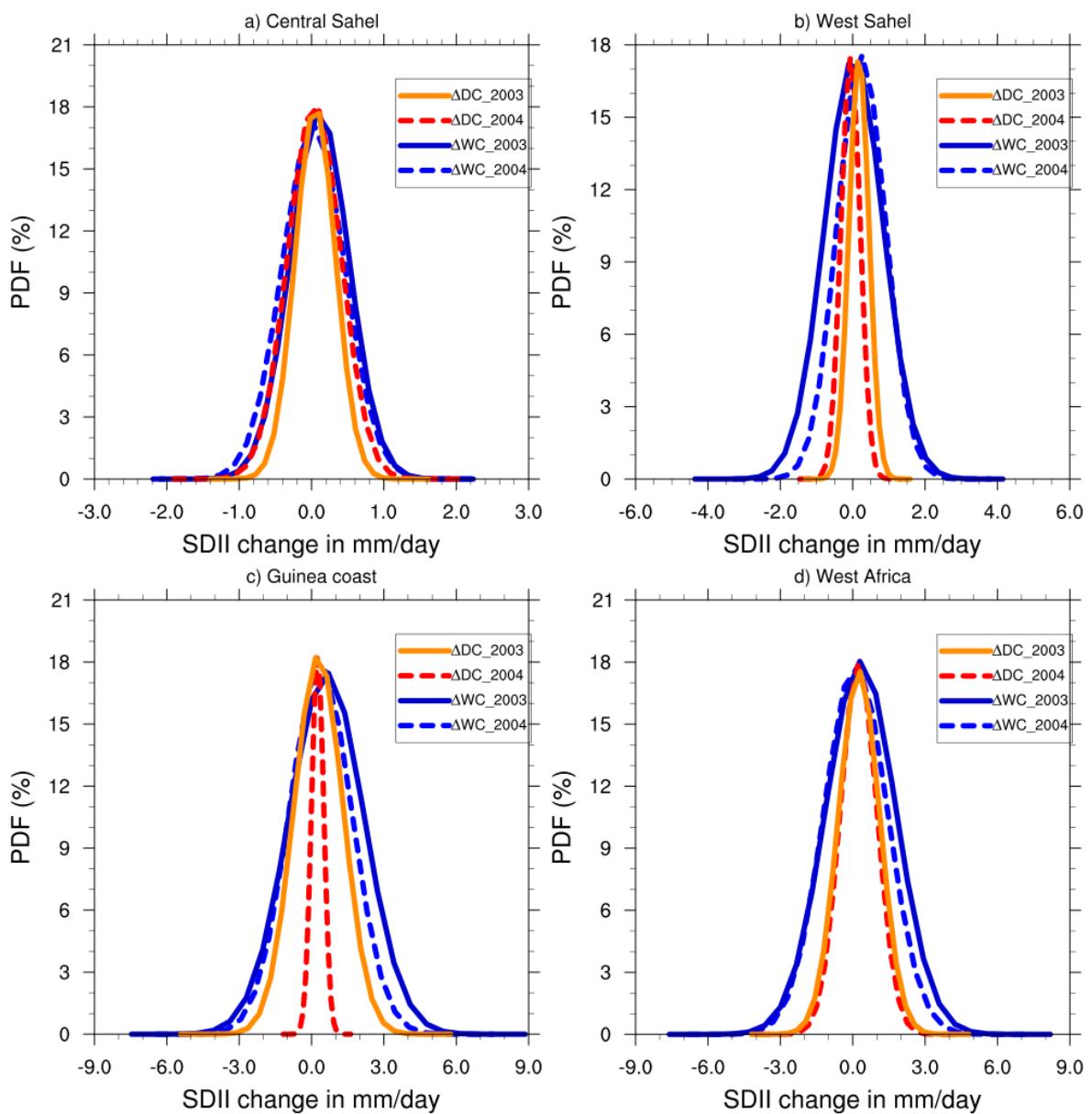
992
993
994
995
996
997 **Figure 5:** Same as Fig. 3 but for the SDII index (in mm.day^{-1}).
998
999
1000
1001
1002
1003
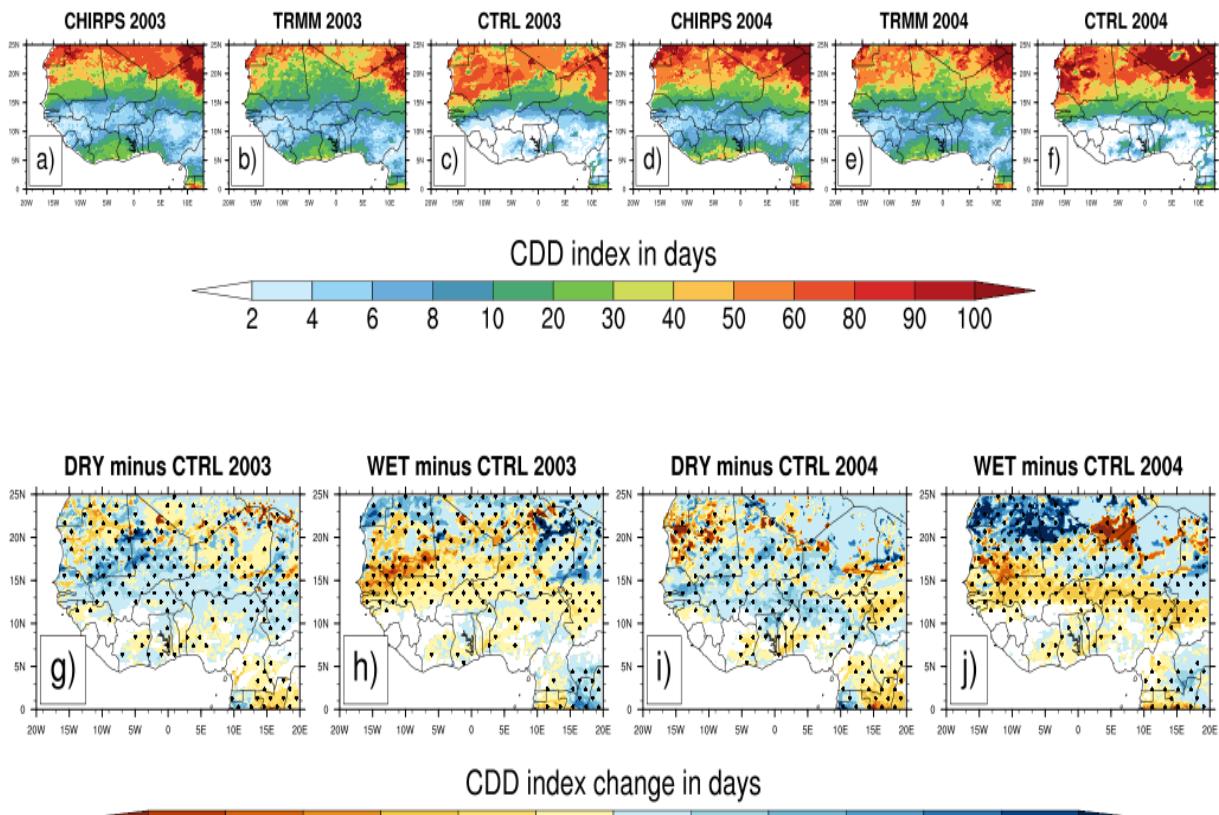
Figure 6: Same as Fig. 2 but for the CDD index (in day).
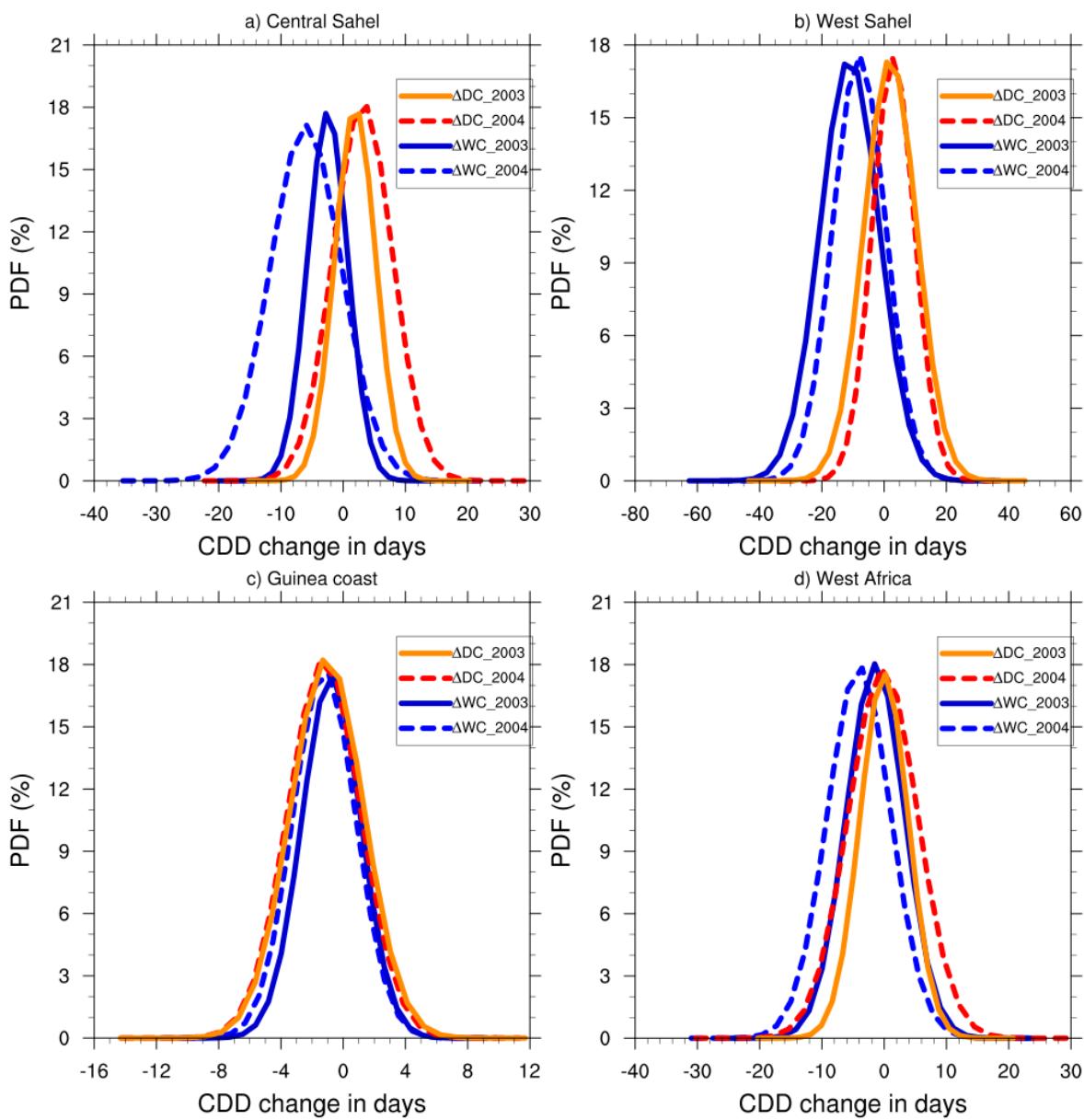
1021
1022
1023

1024   **Figure 7:** Same as Fig. 3 but for the CDD index (in day).

1025
1026
1027
1028
1029
1030
1031
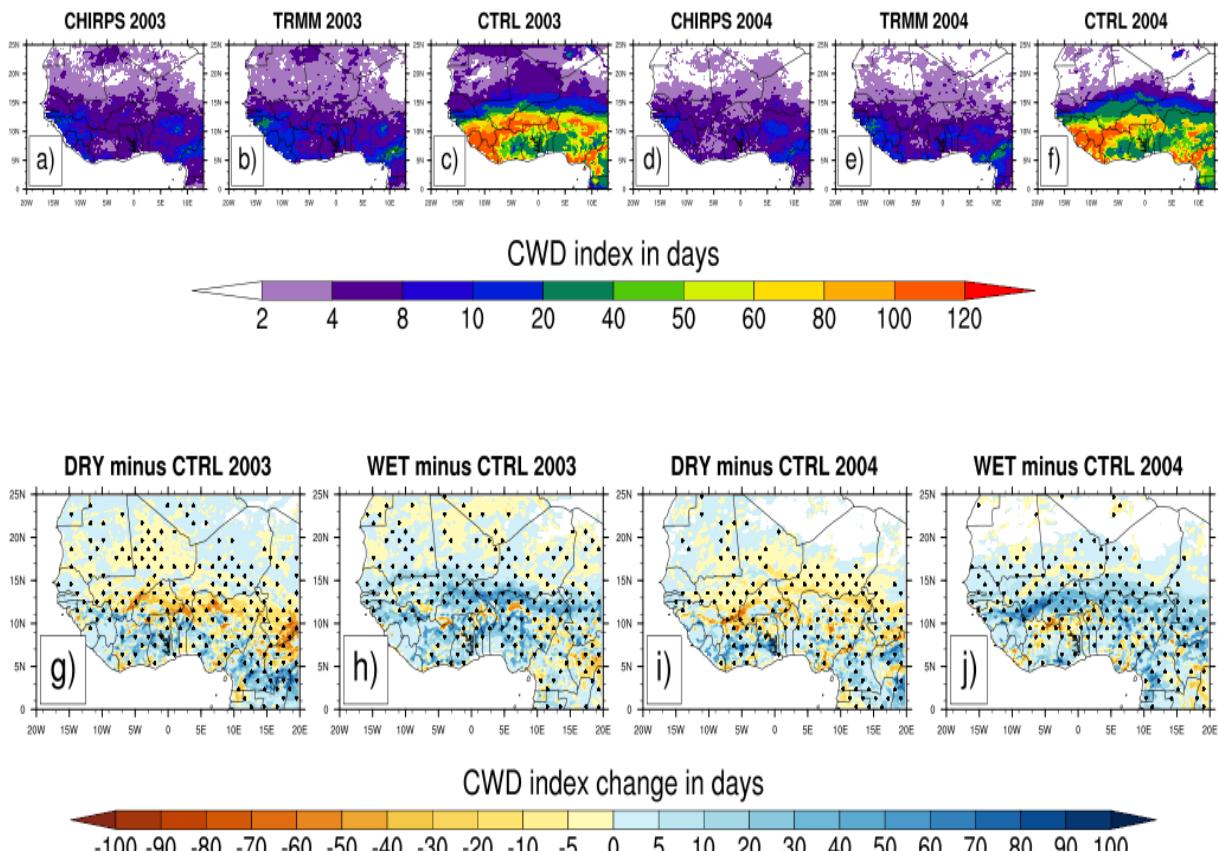
Figure 8: Same as Fig. 2 but for the CWD index (in day).
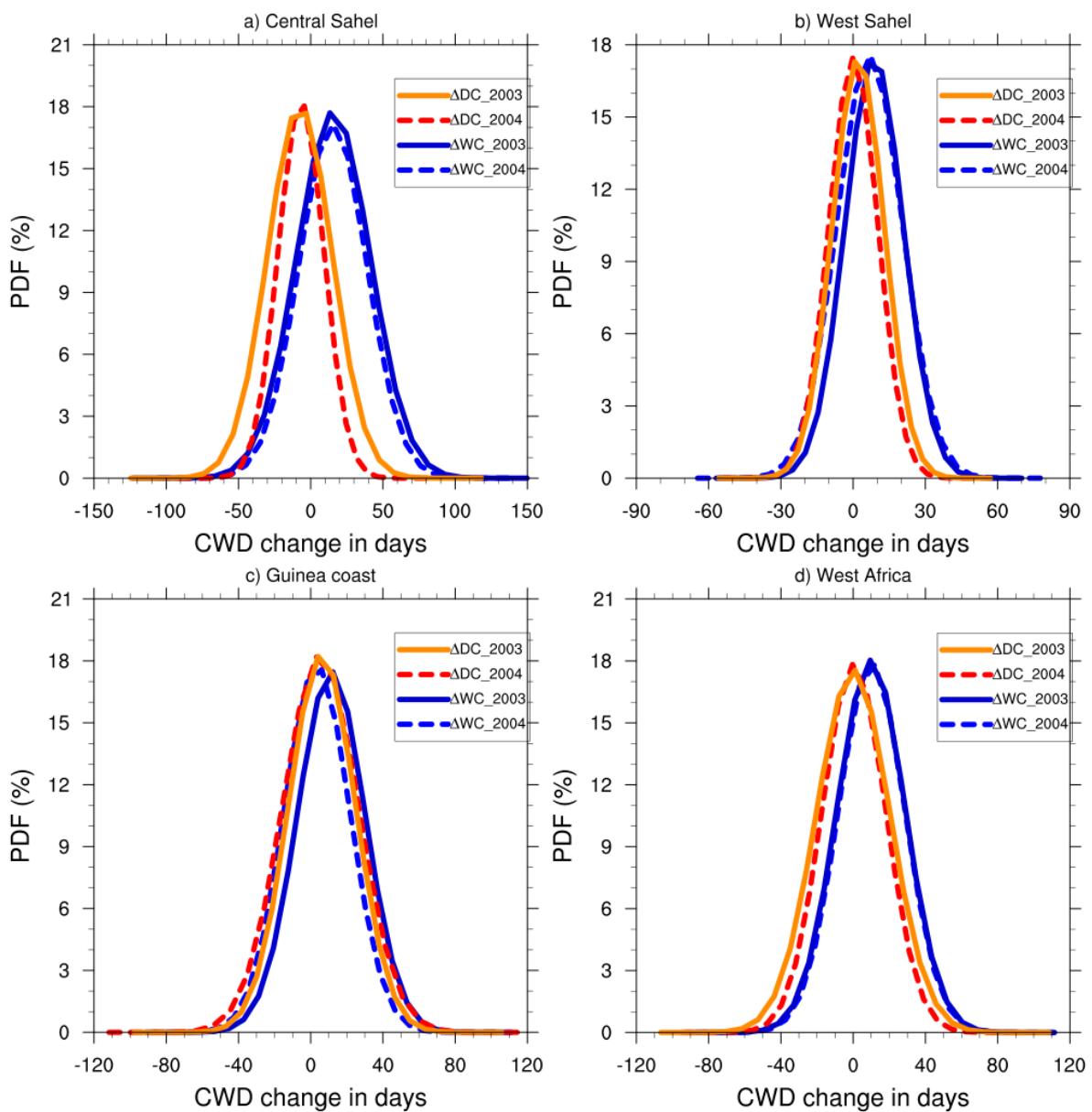
1051
1052

Figure 9: Same as Fig. 3 but for the CWD index (in day).

1053

1054

1055

1056

1057

1058

1059

1060

1061

1062
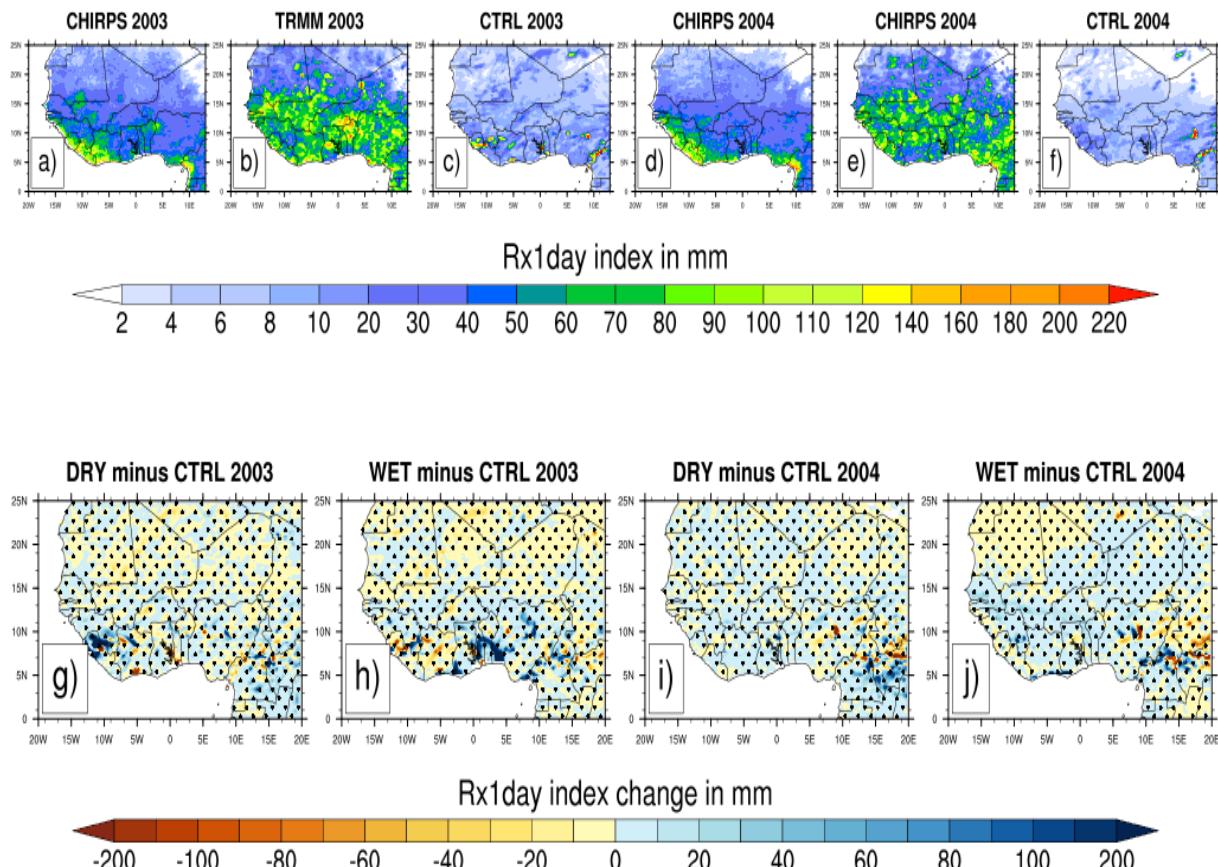
Figure 10: Same as Fig. 2 but for the RX1day index (in mm).
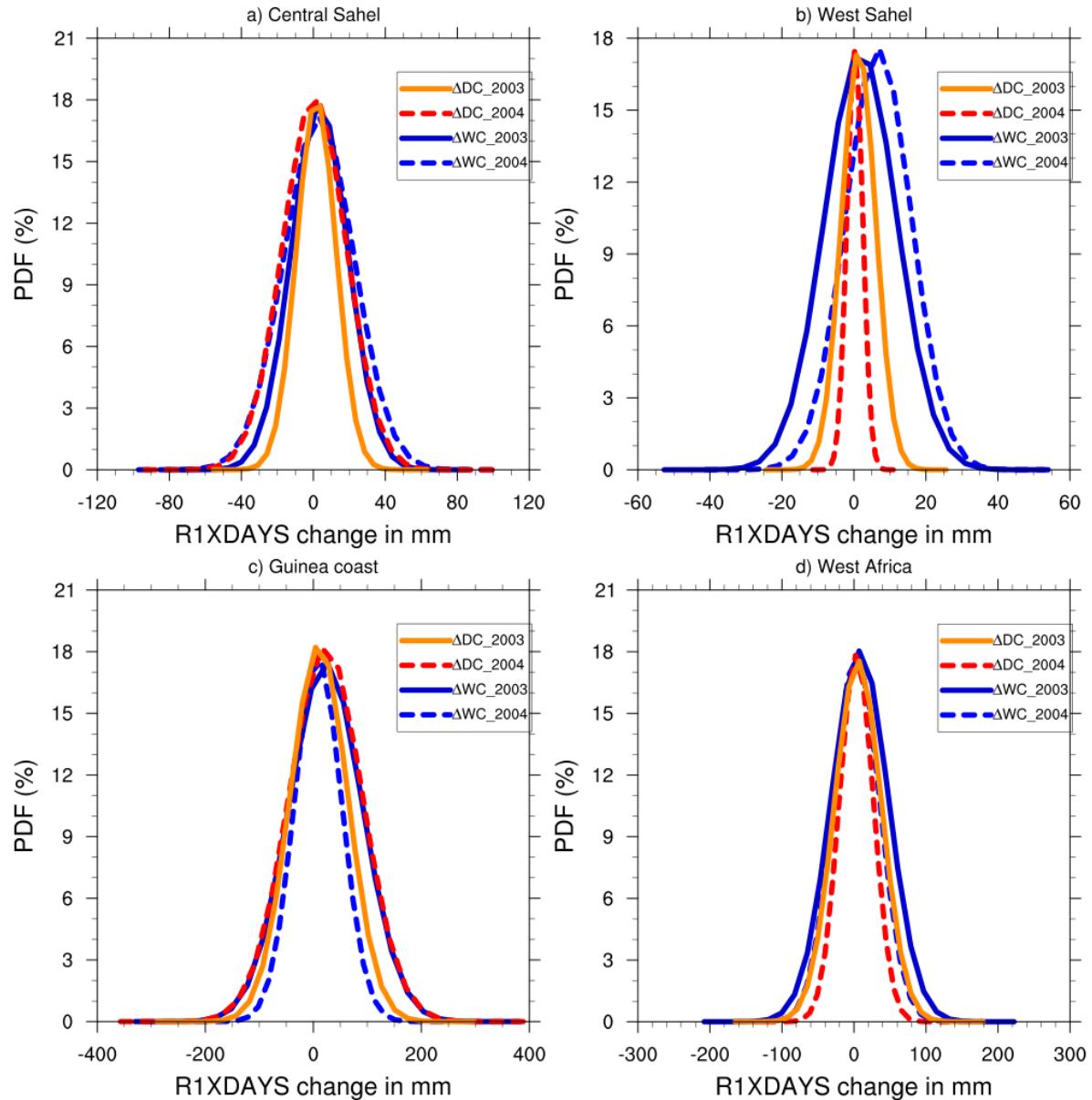
1084   **Figure 11**: Same as Fig. 3 but for the RX1DAY index (in mm).

1085

1086

1087

1088

1089

1090

1091
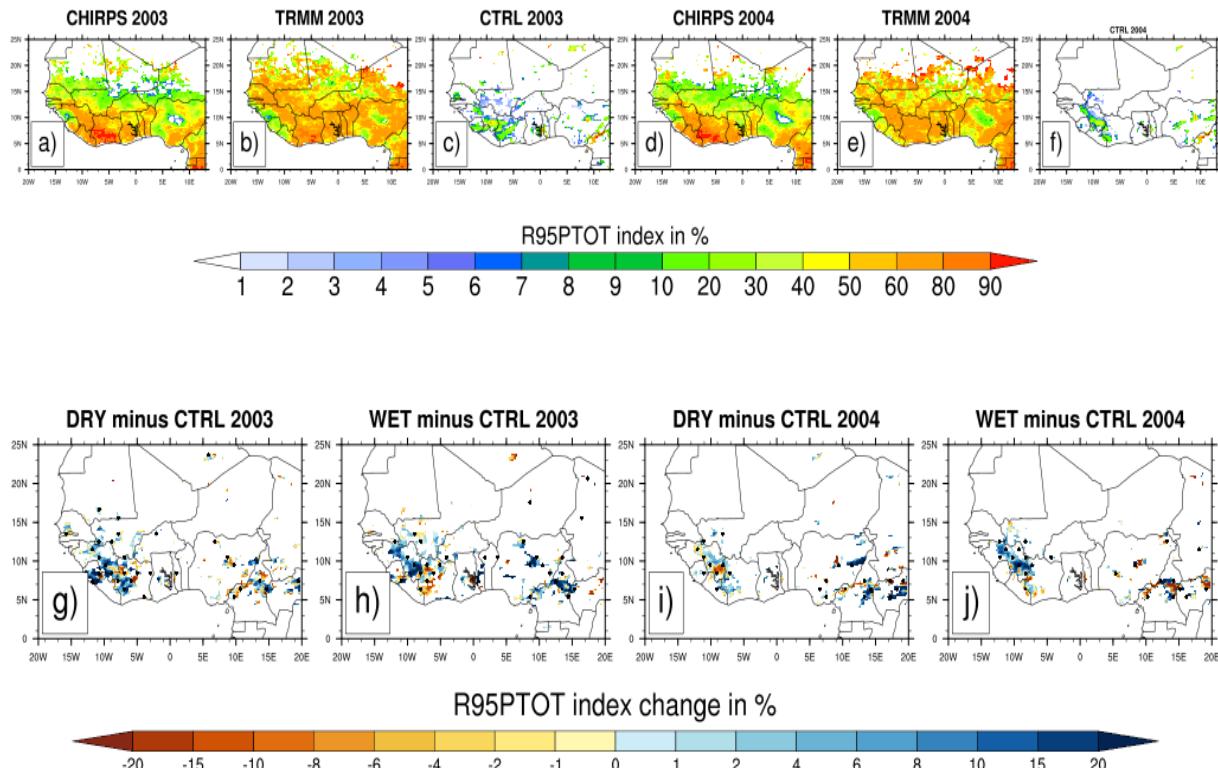
1095 **Figure 12:** Same as Fig. 2 but for the R95pTOT index (in %).

1096
1097
1098
1099
1100
1101
1102
1103
1104
1105
1106
1107
1108
1109
1110
1111

1112
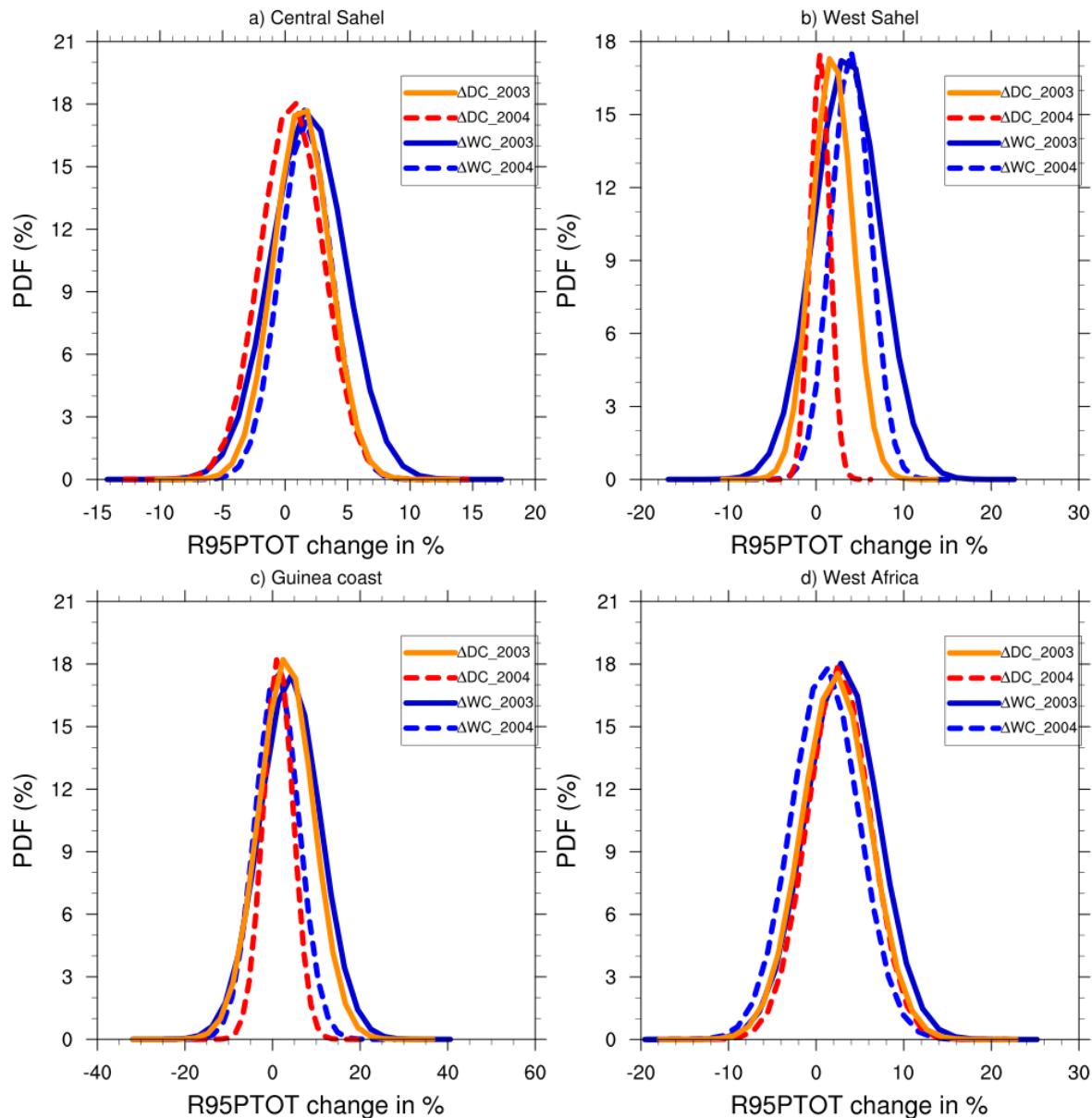
1113

1114 **Figure 13:** Same as Fig. 3 but for theR95pTOT index (in %).

1115

1116

1117

1118

1119

1120

1121

1122

1123
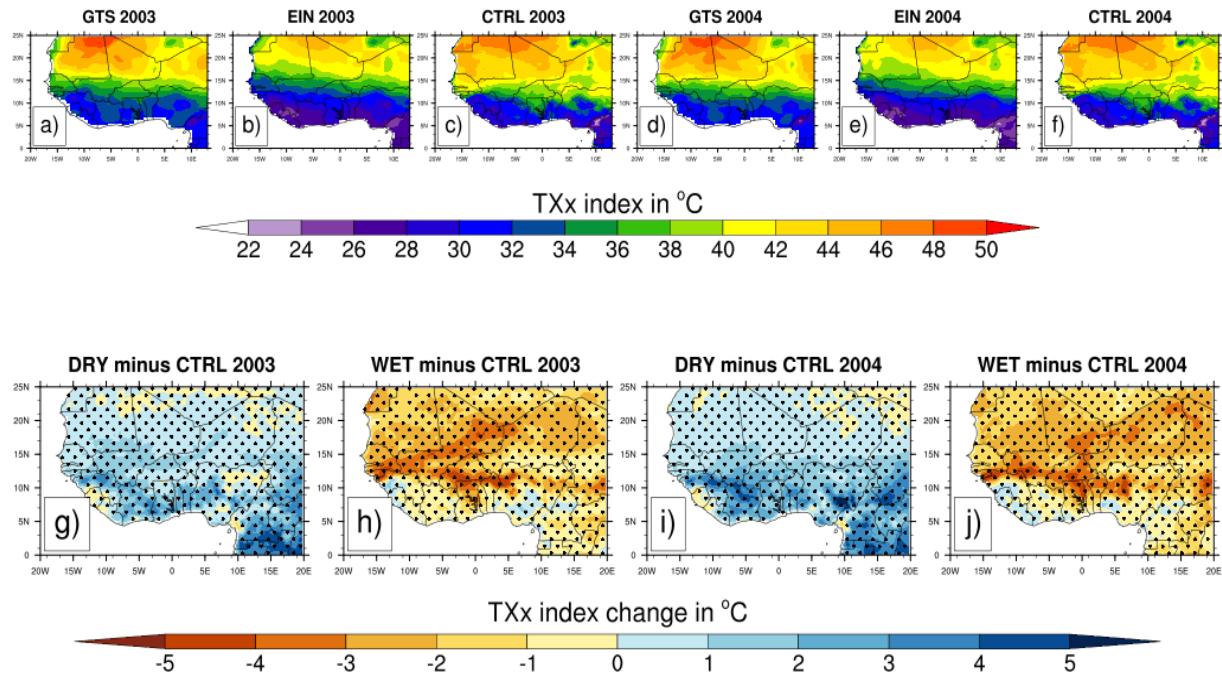
1124

1125 **Figure 14:** The mean maximum value of daily maximum temperature (TXx index in°C) from
1126 GTS observation (a and d) and The EIN reanalysis (b and e) for JJAS 2003 and JJAS 2004
1127 and their corresponding simulated control (CTRL) experiments (c and f) initialized with the
1128 initial soil moisture of the ERA20C reanalysis (first panel) and changes in TXx index in°C
1129 (second panel) for JJAS 2003 and JJAS 2004, from dry (g and i) and wet (h and j)
1130 experiments with respect to the corresponding control experiments. Areas with values passing
1131 the 10% significance test are dotted.

1132
1133
1134
1135
1136
1137
1138
1139
1140
1141
1142
1143
1144

1145
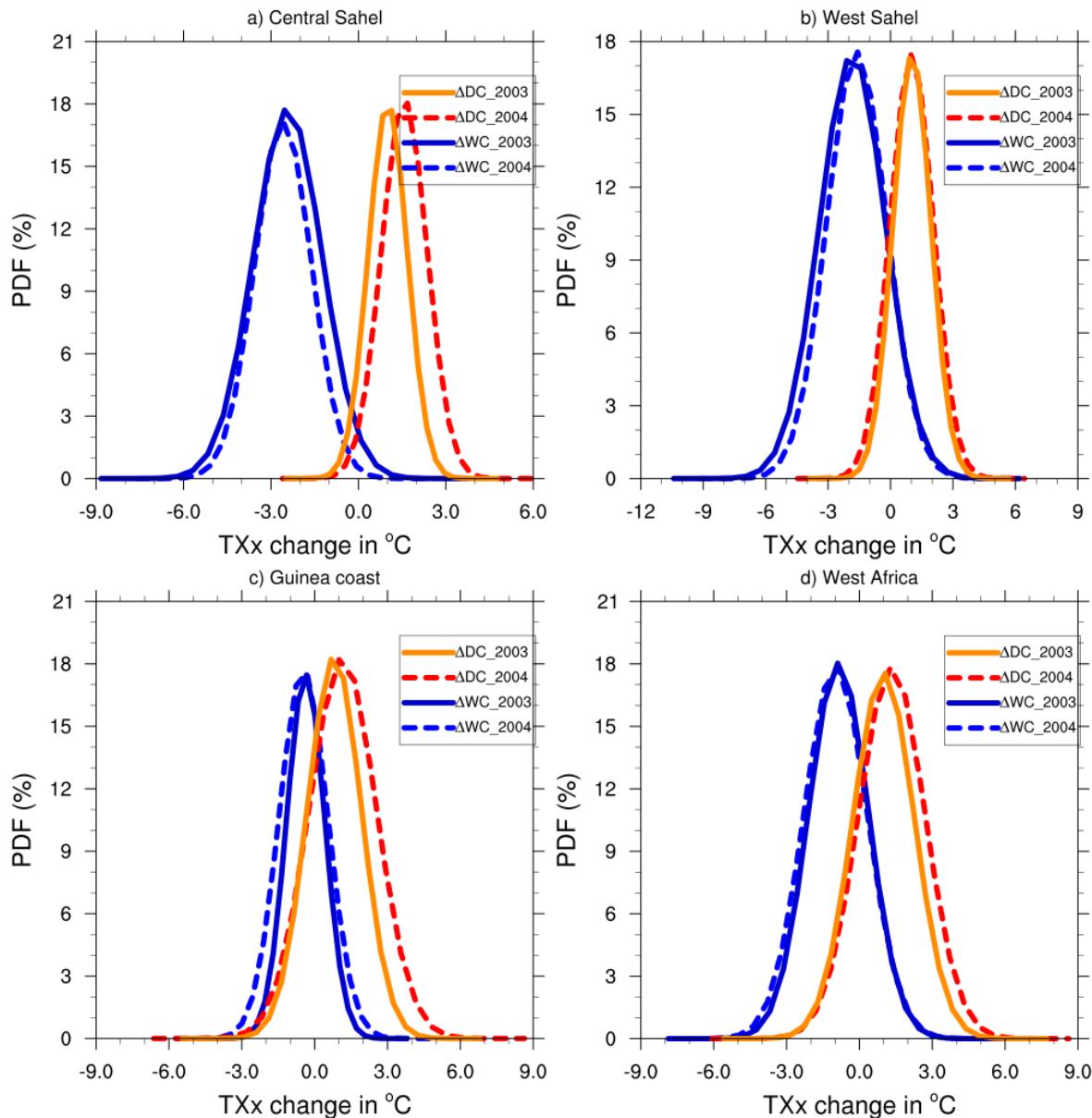
1146
1147

1148 **Figure 15:** PDF distributions (%) of change in maximum value of daily maximum
1149 temperature (TXx index, in°C) for JJAS 2003 and JJAS 2004, over (a) central Sahel , (b)
1150 West Sahel, (c) Guinea and (d) West Africa derived from dry (ΔDC) and wet (ΔWC)
1151 experiments compared to their corresponding control experiment.

1152

1153

1154

1155

1156
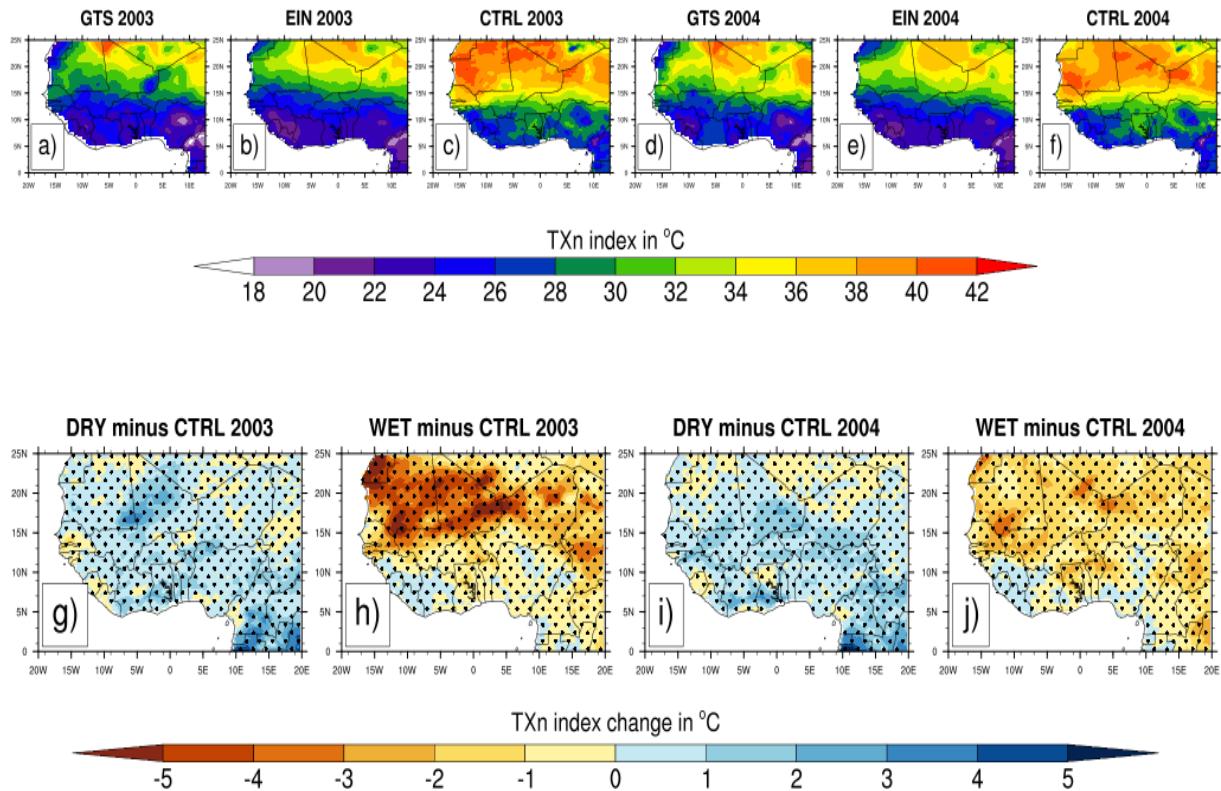
1157
1158
1159

1160 **Figure 16:** Same as Fig. 14 but for the TXn index

1161
1162
1163
1164
1165
1166
1167
1168
1169
1170
1171
1172
1173
1174
1175

1176
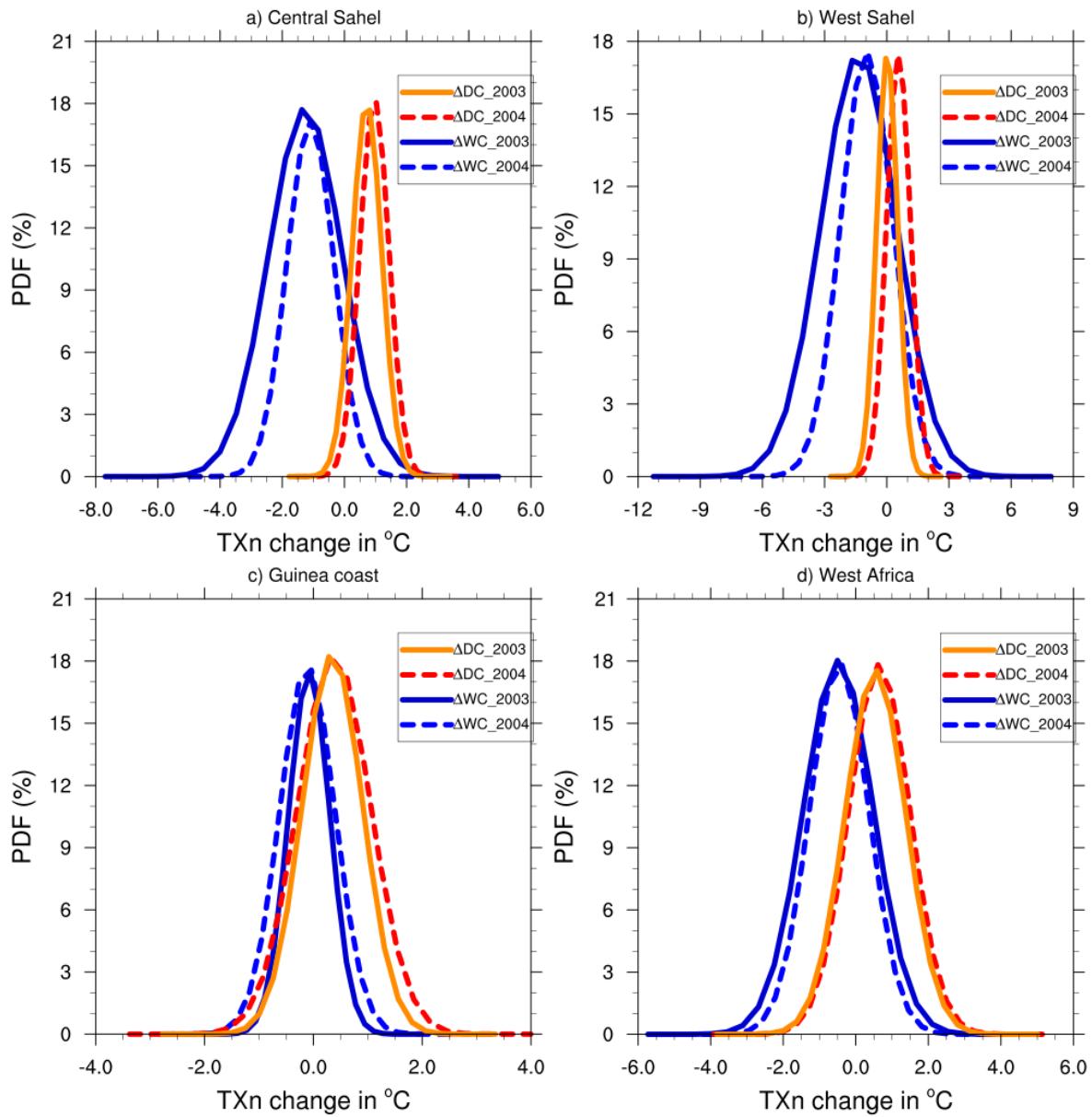
1177
1178
1179
1180

Figure 17: Same as Fig. 15 but for the TXn index.

1182
1183
1184
1185
1186

1187
1188
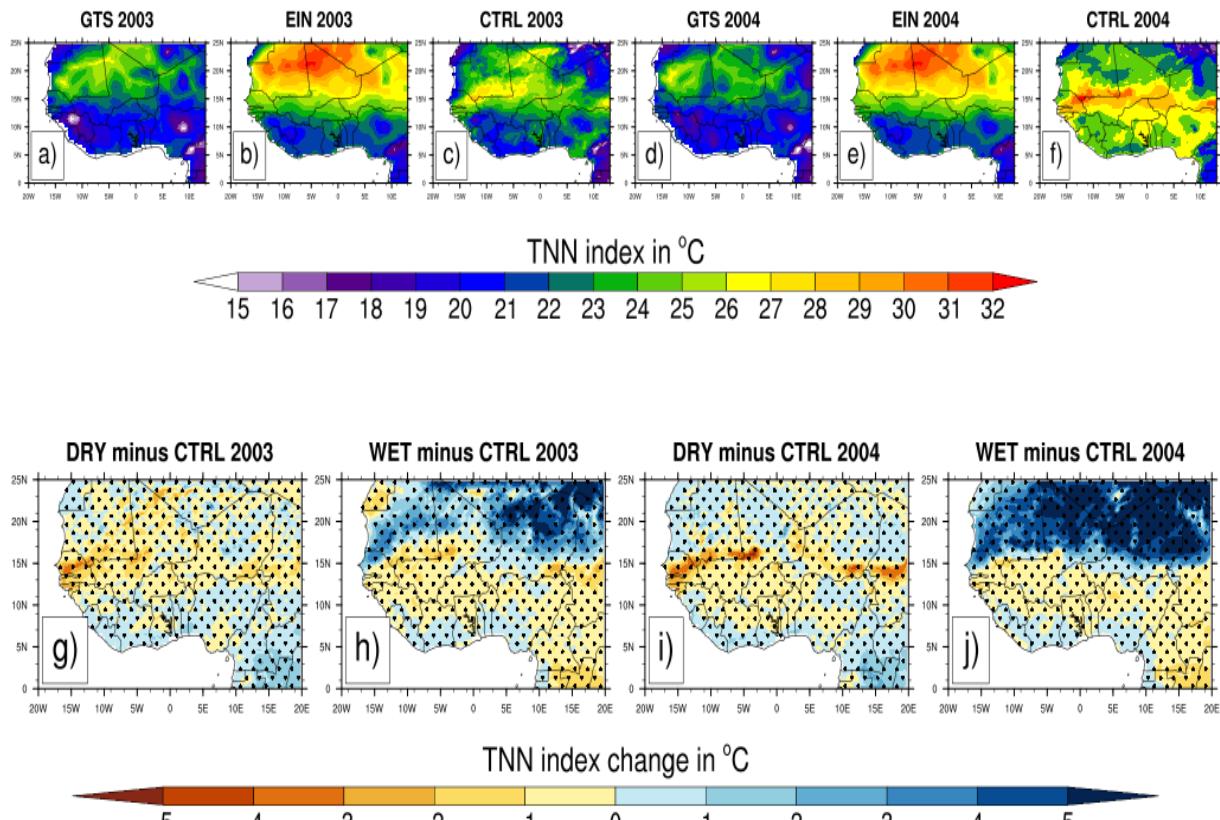
1189
1190
1191

Figure 18: Same as Fig. 14 but for the TNn index.

1193
1194
1195
1196
1197
1198
1199
1200
1201
1202
1203
1204
1205

1206

1207
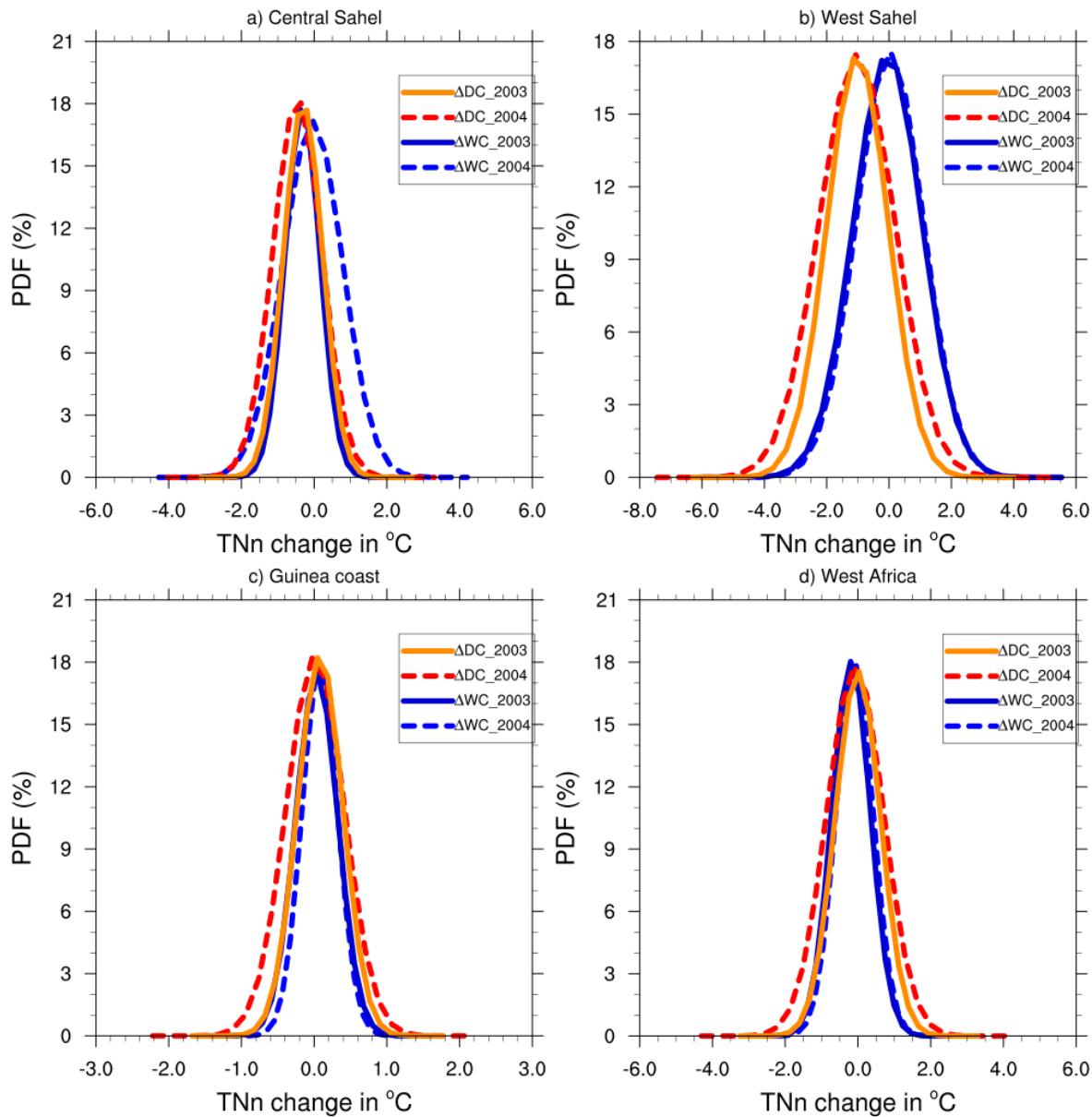
1208

1209

1210

1211

1212 **Figure 19:** Same as Fig. 14 but for the TNn index.

1213

1214

1215

1216
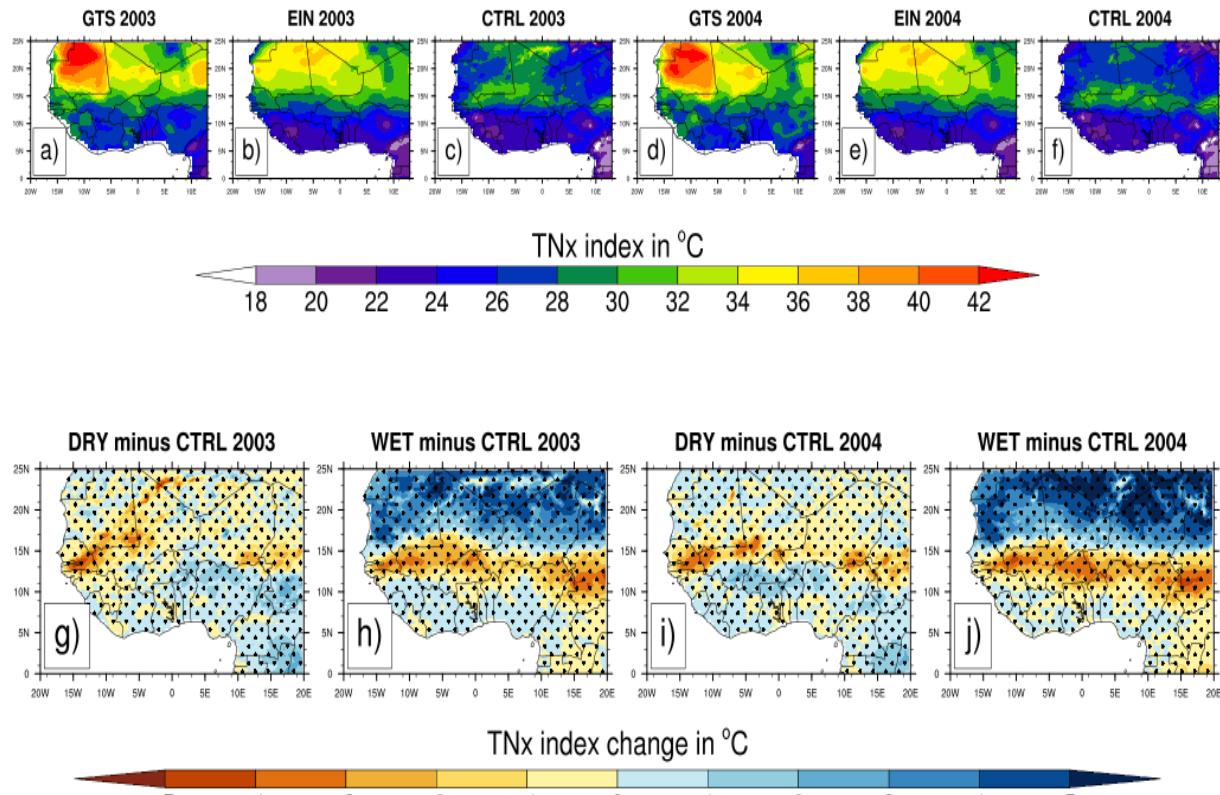
Figure 20: Same as Fig. 14 but for the TNx index
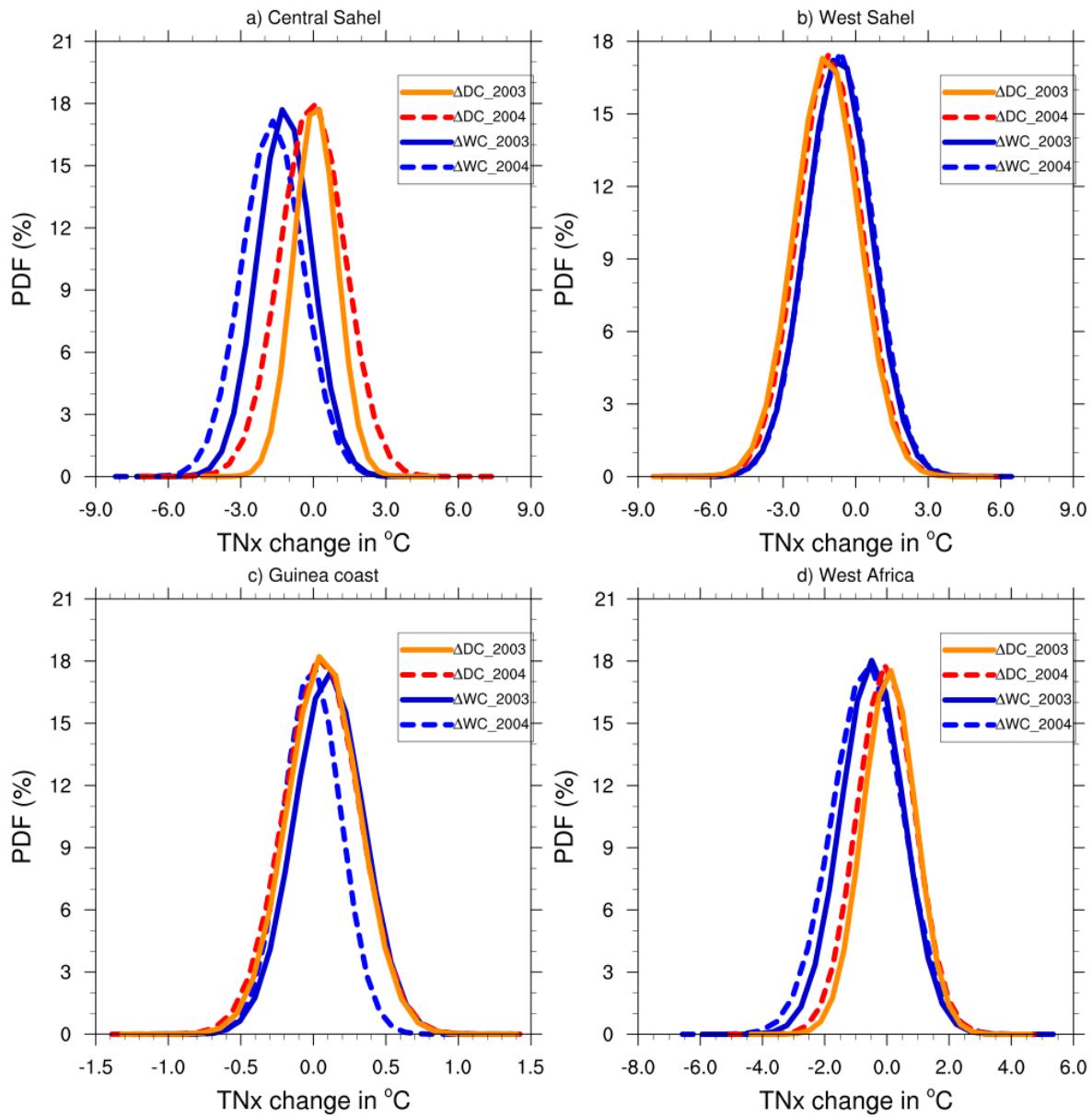
1240   **Figure 21:** Same as Fig. 15 but for the TNx index.